Characterizing Tolerable Disturbances for Transient-State Safety in Power Networks

Yifu Zhang and Jorge Cortés, *Fellow, IEEE*

Abstract—This paper develops methods to compute the set of disturbances on a power network that do not tip the frequency of each bus and the power flow in each transmission line beyond pre-defined bounds. For a linearized AC power network model, we consider scenarios with varying degree of knowledge about the form of the disturbance. We propose a sampling method to provide inner and outer approximations with tunable accuracy of the set of tolerable disturbances. The complexity of computing such set approximations is a function of the number of sampling points. We introduce an error metric to measure the gap between the approximations and design an algorithm that finds, for fixed number of sampling points, the sampling sequence that minimizes its value. Simulations on the IEEE 39-bus power network illustrate our results.

Index Terms—Power networks, transient-state safety, robustness to disturbances, cascading failures.

1 Introduction

Power systems safety is a fundamental aspect of the operation and management of the grid. Ensuring safety has become especially challenging in today's large-scale systems, with uncertainty and variability coming from renewable sources and consumer participation. Transient-state safety refers to the ability of power networks to reach an acceptable state range when subject to disturbances while at the same time respecting operational constraints. Due to the difficulty of explicitly characterizing the form, magnitude, location and duration of disturbances, it is hard to precisely describe their effect on the behavior of power networks during transients. The present work is motivated by the goal of facilitating such understanding using computational tools.

Literature review

System stability refers to the ability to "regain a state of operating equilibrium after being subjected to a physical disturbance, with most system variables bounded so that practically the entire system remains intact [2]". There are two major methods [2], [3] for analyzing stability: time-domain and Lyapunov direct methods. The time-domain method [4], [5], [6] usually refers to the numerical simulation of the system behavior for some specific disturbance. Depending on the numerical solver, this method is able to consider almost any power network model and to precisely depict the state trajectories, provided that the system parameters are accurately known. However, the time-domain method cannot answer question regarding how far the system is from (in)stability and can hardly provide guidelines for control [7]. The Lyapunov direct method [8], [9], [10], [11], [12], focuses on estimating the region of attraction of the system equilibrium using Lyapunov functions to ensure the stability of the power networks without knowing the specific form of the disturbance (provided the initial state lies in the identified region). Most of the direct methods require less simulation/computation time than time-domain methods and, more importantly, are able to provide stability margins and parameter sensitivity analysis. However, due to the difficulty of finding Lyapunov functions, especially for power systems with complex dynamics subject to time-varying disturbances, and the conservativeness required in bounding their evolution, the identified regions of attraction could be coarse approximations of the actual one. In this paper we take the alternative approach of identifying the set of disturbances under which the state of the power system remains within desired bounds during transients. The availability of these descriptions makes it possible to quantify network robustness by, for instance, defining metrics that measure the minimum disturbance that is able to force the system out of the safety region, see e.g., [13], [14]. Such notions are useful in the context of cascading failures analysis and, unlike much of the literature, see e.g., [15], [16], they help identify conditions for triggering initial failures that incorporate the effect of not only network connectivity, but also network dynamics.

Our research here is also related to the literature on the characterization of forward and backward reachability sets, see [17], [18], [19] and, in the context of power systems, [20] for linear dynamics, [21], [22], [23] for nonlinear dynamics with time-varying uncertainty, and [24] for constant uncertainty. Given regions of initial states and possible input signals, a state belongs to the forward reachability set if there exists an initial state and an input signal trajectory that steer the dynamical system to this particular state. Similarly, a state belongs to the backward reachability set if the system can be driven starting from this state into the region with an input trajectory. In general, both types of sets are too difficult to compute precisely, so instead the emphasis is put on constructing accurate inner and outer approximations. An important observation is that reachability set analysis puts the emphasis on characterizing the achievable system states and ensuring that transient trajectories satisfy desired specifications *given* the set of allowable inputs or disturbances. Our emphasis here is entirely complementary: we focus on characterizing the set of disturbances that do not cause the system state to violate the desired specifications.

- *Yifu Zhang and Jorge Cortés are with the Department of Mechanical and Aerospace Engineering, University of California, San Diego.*
  E-mail: {yifuzhang,cortes}@ucsd.edu

A preliminary version appeared as [1] at the American Control Conference.

Statement of contributions

We consider a linearized AC power network subject to multiple disturbances, with each one modeled as amplitude multiplying a time-varying signal, injected at various buses. We distinguish between three cases: when the form of the trajectory is totally known, partially known, or totally unknown but bounded. A disturbance is tolerable for the transient-state safety of the power network if the frequency of each bus and the power flow in each transmission line still remain in their respective bounds during a given period of time. Our main goal is to design efficient ways of computing the transient-state tolerableness set consisting of all such classes of disturbances. Our first contribution shows that all three transient-state tolerableness sets can be equivalently expressed in a unified way that contain infinitely many constraints. The second contribution develops a sampling method to approximate these sets by synthesizing inner and outer approximations. The inner approximation is computed by sampling and tightening the constraints at finite discrete-time instants. We use the network dynamics to upper and lower bound the evolution of state signals and show that satisfying the constraints at these finite instants ensures in fact that all constraints are respected at all times. The outer approximation comes from using only a finite number of the constraints appearing in the original transient-state tolerableness set. We show that, as the number of sampling points increases, the approximation sets converge to the real transient-state tolerableness set. Our third contribution consists of defining a metric to measure the approximation gap by estimating the region difference between the approximations and the real set. We characterize the sampling sequence that, for a fixed number of sampling points, results in the minimal gap of the approximations and design an algorithm to find it by efficiently adjusting the positions of the sampling points. Finally, we illustrate our results on the IEEE 39-bus power system by showing the inner and outer approximations of the three tolerableness sets.

2 Preliminaries

Here we introduce basic notation and mathematical notions.

Notation

Let $\mathbb{R}$, $\mathbb{R}_{>}$, $\mathbb{R}_{\geqslant}$ and $\mathbb{N}$ denote the set of real, strictly positive real, non-negative real and natural numbers, respectively. Variables are assumed to belong to the Euclidean space if not specified otherwise. For $p,q \in \mathbb{N}$, let $[p,q]_{\mathbb{N}} \triangleq \{x \in \mathbb{N} \mid p \leqslant x \leqslant q\}$. We denote by $a \leqslant b$ $(<,\geqslant,>)$ the element-wise set of inequalities for vectors $a,b \in \mathbb{R}^n$. We let $\mathbf{1}_n$ and $\mathbf{0}_n$ in $\mathbb{R}^n$ denote the vector of all ones and zeros, respectively. Let $I_n \in \mathbb{R}^{n\times n}$ denote the identity matrix and $\mathrm{diag}(a) \in \mathbb{R}^{n\times n}$ be the diagonal matrix whose diagonal is given by the elements of $a \in \mathbb{R}^n$. For $A \in \mathbb{R}^{m\times n}$, let $[A]_i$ and $[A]_{i,j}$ denote its ith row and (i,j)th element, respectively, and $|A| \in \mathbb{R}^{m\times n}$ the matrix whose entries are the absolute values of the entries of A. Given $\Sigma \subset \mathbb{R}^n$, we let Σ_{cl} denote its closure.

Algebraic graph theory

We review basic notions from algebraic graph theory from [25], [26]. An undirected graph is a pair $\mathcal{G} = (\mathcal{I},\mathcal{E})$, where $\mathcal{I} = \{1,\dots,n\}$ is the vertex set and $\mathcal{E} = \{e_1,\dots,e_m\} \subseteq \mathcal{I}\times\mathcal{I}$ is the edge set. A path is an ordered sequence of vertices such that any pair of consecutive vertices in the sequence is an edge of the graph. A graph is connected if there exists a path between any two vertices. Two nodes are neighbors if there exists an edge linking them. Let $\mathcal{N}(i)$ denote the set of neighbors of node i. For each edge $e_\alpha \in \mathcal{E}$ with vertices i,j, the orientation procedure consists of choosing either i or j to be the positive end of e_α and the other vertex to be the negative end. The incidence matrix $D = (d_{\alpha i}) \in \mathbb{R}^{m\times n}$ associated with $\mathcal{G}$ is defined as

$$d_{\alpha i} = \begin{cases} 1 & \text{if } i \text{ is the positive end of } e_\alpha, \\ -1 & \text{if } i \text{ is the negative end of } e_\alpha, \\ 0 & \text{otherwise.} \end{cases}$$

Set limit

We introduce basic definitions from set theory [27]. Given a sequence of sets $\{A_k\}_{k=1}^{\infty}$, define

$$\liminf_{k\to\infty} A_k \triangleq \bigcup_{k\geqslant 1}\bigcap_{j\geqslant k} A_j, \ \limsup_{k\to\infty} A_k \triangleq \bigcap_{k\geqslant 1}\bigcup_{j\geqslant k} A_j.$$

It holds that $\liminf_{k\to\infty} A_k \subseteq \limsup_{k\to\infty} A_k$. Furthermore, if $\liminf_{k\to\infty} A_k = \limsup_{k\to\infty} A_k = A$, then we say the limit of $\{A_k\}_{k=1}^{\infty}$ exists and is A. In shorthand notation, we write $A_k \to A$. For a set C and two set sequences $\{B_k\}_{k=1}^{\infty}$ and $\{C_k\}_{k=1}^{\infty}$, if $C \subseteq B_k \subseteq C_k$ (resp. $C_k \subseteq B_k \subseteq C$) for all $k \geqslant 1$, and $C_k \to C$, then $B_k \to C$.

3 Problem Statement

This section describes the problem of interest. We start by describing the model for the power grid and its dynamics, and then define the desired safety criteria against disturbances.

3.1 Power network dynamics

Following [28], [29], [30], the power network model structure is encoded by a connected undirected graph $\mathcal{G} = (\mathcal{I},\mathcal{E})$, where $\mathcal{I}$ corresponds to the n buses and $\mathcal{E}$ represents the m transmission lines. We denote by $P = [P_1,P_2,\dots,P_n]^T \in \mathbb{R}^n$, $\Theta = [\theta_1,\theta_2,\dots,\theta_n]^T \in \mathbb{R}^n$, and $\Omega = [\omega_1,\omega_2,\dots,\omega_n]^T \in \mathbb{R}^n$, respectively, the network power injection, the voltage angle, and the frequency vectors. In each case, the ith component of the vector corresponds to the ith node. The linearized power network dynamics are then described by the following equations: for each $i \in \mathcal{I}$,

$$\dot{\theta}_i(t) = \omega_i(t), \tag{1a}$$

$$M_i\dot{\omega}_i(t) = -E_i\omega_i(t) - \sum_{j\in\mathcal{N}(i)} b_{ij}(\theta_i(t)-\theta_j(t)) + P_i(t), \tag{1b}$$

where $M_i \geqslant 0$ (resp. $E_i > 0$) is the moment inertia (resp. damping parameter or droop coefficient) at node i, and b_{ij} is the susceptance of the transmission line between node i and j. Let $D \in \mathbb{R}^{m\times n}$ be the incidence matrix corresponding to an arbitrary orientation of the graph $\mathcal{G}$ and define $\Lambda(t) \triangleq D\Theta(t) \in \mathbb{R}^m$ as the voltage angle difference between every two neighboring nodes. We rewrite the dynamics (1) in compact form [31] as

$$\begin{bmatrix} \dot{\Lambda}(t) \\ M\dot{\Omega}(t) \end{bmatrix} = \begin{bmatrix} \mathbf{0}_{m\times m} & D \\ -D^T Y_b & -E \end{bmatrix} \begin{bmatrix} \Lambda(t) \\ \Omega(t) \end{bmatrix} + \begin{bmatrix} \mathbf{0}_m \\ P(t) \end{bmatrix}, \tag{2}$$

where $M \triangleq \mathrm{diag}([M_1,M_2,\dots,M_n]) \in \mathbb{R}^{n\times n}$, $E \triangleq \mathrm{diag}([E_1,E_2,\dots,E_n]) \in \mathbb{R}^{n\times n}$, $Y_b \triangleq \mathrm{diag}\{b_{ij}\} \in \mathbb{R}^{m\times m}$. Notice that the power flow can be represented by $Y_b\Lambda(t)$. Throughout the paper, we use (2) to describe the power network dynamics.

3.2 Disturbance modeling and safety criteria

We are interested in understanding how disturbances in the power injection affect the transient-state safety of the power network. For system (2) with an arbitrary initial state $(\Lambda(0),\Omega(0))$ and a known nominal power injection $P^{\text{nom}}(t)\in\mathbb{R}^n$, we consider the case where an additional unknown power disturbance $P^{\text{dist}}(t)\in\mathbb{R}^n$ is injected starting at time 0, i.e.,

$$P(t)=P^{\text{nom}}(t)+P^{\text{dist}}(t),\quad \forall t\geqslant 0. \tag{3}$$

Such additive disturbances model the mismatch between predicted and actual power injection in power systems and might arise, for instance, from variability in the load consumption or uncertainty in power generation caused by, e,.g., renewable energy sources. As safety criteria, we consider the following:

(i) *Transient-state frequency bound:* Given $0\leqslant t_1<t_2$, the voltage frequency $\Omega(t)$ satisfies

$$\Omega^{\min}<\Omega(t)<\Omega^{\max},\quad \forall t\in[t_1,t_2].$$

(ii) *Transient-state power flow bound:* Given $0\leqslant t_1<t_2$, the power flow $Y_b\Lambda(t)$ satisfies

$$F^{\min}<Y_b\Lambda(t)<F^{\max},\quad \forall t\in[t_1,t_2].$$

Depending on how much is known about the form of the disturbance signal P_{dist}, we provide different definitions of what it means for a disturbance to be tolerable by the system, i.e., not disrupt its transient-state safety. We consider three increasingly realistic cases:

(a) *Precisely known trajectory form:* the amplitude of the disturbance is unknown but its trajectory form is precisely known,

$$P^{\text{dist}}(t)=B\,\text{diag}(\zeta^{\text{pre}}(t))K^{\text{pre}},\quad \forall t\geqslant 0, \tag{4}$$

where $K^{\text{pre}}\in\mathbb{R}^s$ denotes the amplitude; $\zeta^{\text{pre}}(t)\in\mathbb{R}^s$ is an integrable function that stands for the trajectory form; $\text{diag}\,(\zeta^{\text{pre}}(t))$ is a shorthand notation for the diagonal matrix $\text{diag}\,(\zeta^{\text{pre}}(t))\in\mathbb{R}^{s\times s}$, and $B\in\mathbb{R}^{n\times s}$ is a constant matrix whose elements are either 0 or 1, representing the buses where the elements of $\text{diag}\,(\zeta^{\text{pre}}(t))\,K^{\text{pre}}$ are injected. The transient-state tolerableness set is then defined as

$$\Psi^{\text{pre}}\triangleq\left\{K^{\text{pre}}\;\middle|\;\text{(i)-(ii) hold for (2) under (3) and (4)}\right\} \tag{5}$$

Clearly, if K^{pre} lies in Ψ^{pre}, then the disturbance $P^{\text{dist}}(t)$ with amplitude K^{pre} does not violate the transient-state requirements.

(b) *Partially known trajectory form:* the amplitude is unknown and the trajectory form is partially known, in the sense that a nominal trajectory form together with an estimation error bound are available. Formally,

$$P^{\text{dist}}(t)=B\,\text{diag}\,(\zeta^{\text{par}})\,K^{\text{par}}, \tag{6a}$$
$$\zeta^{\text{par}}(t)=\zeta^{\text{nom}}(t)+\zeta^{\text{err}}(t), \tag{6b}$$

where $\zeta^{\text{nom}}(t)\in\mathbb{R}^s$ is known and $\zeta^{\text{err}}(t)\in\mathbb{R}^s$ is bounded component-wise by a known vector $\alpha\in\mathbb{R}^s$. For convenience, we define $\mathbf{Z}(\alpha)\triangleq\left\{\zeta\;\middle|\;|\zeta_i(t)|\leqslant\alpha_i,\ \forall i\in[1,s]_{\mathbb{N}},\ \forall t\in[t_1,t_2]\right\}$. The transient-state tolerableness set is then defined as

$$\Psi^{\text{par}}\triangleq\left\{K^{\text{par}}\;\middle|\;\forall\zeta^{\text{err}}\in\mathbf{Z}(\alpha),\ \text{(i)-(ii) hold for (2) under (3) and (6)}\right\}. \tag{7}$$

The interpretation of this set is that, if the amplitude K^{par} belongs to Ψ^{par}, then the transient-state requirements (i)-(ii) are satisfied under the disturbance $P^{\text{dist}}(t)$ no matter how the evolution of the unknown trajectory estimation error $\zeta^{\text{err}}(t)$ (as long as it remains bounded by α). Notice that if $\alpha=\mathbf{0}_s$ and $\zeta^{\text{nom}}=\zeta^{\text{pre}}$, then $\Psi^{\text{par}}=\Psi^{\text{pre}}$. We still deal with the case of precisely known trajectory form independently as its treatment sets the basis for generalization to the other two, more complicated, cases.

(c) *Unknown trajectory form:* both the amplitude and the trajectory form of the disturbance are unknown. To define the transient-state tolerableness set in this case, we consider the magnitude, rather than the amplitude, of the disturbance. Formally,

$$P^{\text{dist}}(t)=BK^{\text{unk}}(t). \tag{8}$$

We define the set of disturbances bounded by $R\in\mathbb{R}^s$ as $\mathbf{P}(R)\triangleq\left\{K^{\text{unk}}\;\middle|\;|K_i^{\text{unk}}(t)|\leqslant R_i,\ \forall i\in[1,s]_{\mathbb{N}},\ \forall t\in[t_1,t_2]\right\}$. The transient-state tolerableness set is then

$$\Psi^{\text{unk}}\triangleq\left\{R\geqslant\mathbf{0}_s\;\middle|\;\forall K^{\text{unk}}\in\mathbf{P}(R),\ \text{(i)-(ii) hold for (2) under (3) and (8)}\right\}. \tag{9}$$

The interpretation of this set is that, if the magnitude bound R belongs to Ψ^{unk}, then the transient-state requirements (i)-(ii) are satisfied under the disturbance $P^{\text{unk}}(t)$ no matter its evolution (as long as it magnitude is bounded by R).

Our goal is to provide formal descriptions of the transient-state tolerableness sets in each of the cases (a)-(c). Given the complexity of obtaining exact descriptions of these sets, we focus on developing inner and outer approximations of them with tunable accuracy. Our strategy to assess the impact of disturbances on system trajectories over the time interval of interest is to consider a finite set of sampling points, ensure certain bounds are satisfied by the trajectories at these points, and reason to ensure that no violations occur in between the sampling points. Figure 1 illustrates the main ideas behind our forthcoming discussion.

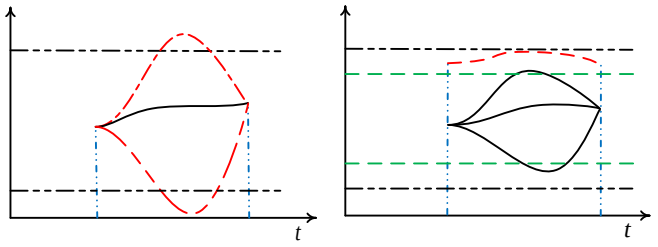

Figure 1. Illustration of our strategy to develop approximations of the transient-state tolerableness sets. In this example, we describe conditions under which a one-dimensional signal trajectory stays within the horizontal black dashed bounds in a time interval determined by the two sampling points. In plot (a), we only require the value of the signal to lie within the bounds at two sampling points, which leads to an outer approximation, as some trajectories (red dashed lines) may exceed the bounds within the time interval. In plot (b), we employ a similar strategy, but require the two terminal values to lie within some stricter bounds, denoted by horizontal green dashed lines, whose positions are determined by knowledge about the signal derivative inside the interval. This allows us to guarantee that the whole trajectory does not exceed the black dashed bounds at any time within the interval. This leads to an inner approximation, as there may be trajectories (e.g., the red dashed one) whose terminal values are not in the stricter green bounds but also stay within the black dashed bounds at all times.

Remark 3.1. *(Time interval selection).* The initial time t_1 is typically the starting time of the disturbance, $t_1=0$. We assume the terminal time t_2 is specified by a system operator based on desired time horizons over which the network performance must meet

certain specifications. In general, the time when the system reaches steady state after the disturbance depends on the disturbance itself, the network connectivity, and the network dynamics in a complex way. The work [2] shows that in transient stability studies t_2 =3 to 5s, and it may extend to 10 to 20s for very large systems with dominant inter-area swing dynamics. •

4 Transformation of the transient-state tolerableness sets

In this section, we show how the transient-state tolerableness sets defined in Section 3.2 can be expressed in a way that shares the same structure across all three cases. This allows for a unified treatment of all cases later.

In our treatment, we consider the case where all buses have strictly positive inertias so that the diagonal matrix M in (2) is invertible. Under the input (3), the dynamics can be written as

$$\dot{x}(t) = Ax(t) + \begin{bmatrix} \mathbf{0}_m \\ M^{-1}P(t) \end{bmatrix}, \tag{10}$$

where

$$x(t) = \begin{bmatrix} \Lambda(t) \\ \Omega(t) \end{bmatrix},\ A = \begin{bmatrix} \mathbf{0}_{m\times m} & D \\ -M^{-1}D^T Y_b & -M^{-1}E \end{bmatrix}.$$

Solving (10), one has

$$x(t) = e^{At}x_0 + \int_0^t e^{A(t-\tau)} \begin{bmatrix} \mathbf{0}_m \\ M^{-1}P(\tau) \end{bmatrix} \mathrm{d}\tau, \tag{11}$$

where $x_0 \triangleq [\Lambda^T(0)\ \Omega^T(0)]^T$. Denoting

$$\begin{aligned} S(t,x_0,P^{\mathrm{nom}}) &\triangleq e^{At}x_0 + \int_0^t e^{A(t-\tau)} \begin{bmatrix} \mathbf{0}_m \\ M^{-1}P^{\mathrm{nom}}(\tau) \end{bmatrix} \mathrm{d}\tau, \\ V(t,\zeta) &\triangleq \int_0^t e^{A(t-\tau)} \begin{bmatrix} \mathbf{0}_{m\times s} \\ M^{-1}B\,\mathrm{diag}\,(\zeta(\tau)) \end{bmatrix} \mathrm{d}\tau, \\ x^{\max} &\triangleq \begin{bmatrix} \Omega^{\max} \\ Y_b^{-1}F^{\max} \end{bmatrix},\ x^{\min} \triangleq \begin{bmatrix} \Omega^{\min} \\ Y_b^{-1}F^{\min} \end{bmatrix}, \end{aligned} \tag{12}$$

one has that in the case (a) of precisely known trajectory form, the state response can be re-written as $x(t) = S(t,x_0,P^{\mathrm{nom}}) + V(t,\zeta^{\mathrm{pre}})K^{\mathrm{pre}}$, and hence the transient-state tolerableness set takes the form

$$\begin{aligned} \Psi^{\mathrm{pre}} = \Big\{ K^{\mathrm{pre}} \,\Big|\, & x^{\min} < S(t,x_0,P^{\mathrm{nom}}) \\ & + V(t,\zeta^{\mathrm{pre}})K^{\mathrm{pre}} < x^{\max},\ \forall t \in [t_1,t_2] \Big\}. \end{aligned} \tag{13}$$

Based on this expression, it is easy to check whether a given amplitude K^{pre} belongs to Ψ^{pre}. However, in cases (b) and (c), one has

$$\begin{aligned} \Psi^{\mathrm{par}} = \{ & K^{\mathrm{par}} \,|\, x^{\min} < S(t,x_0,P^{\mathrm{nom}}) + V(t,\zeta^{\mathrm{nom}})K^{\mathrm{par}} \\ & + V(t,\zeta^{\mathrm{err}})K^{\mathrm{par}} < x^{\max},\ \forall \zeta^{\mathrm{err}} \in \mathbf{Z}(\alpha),\ \forall t \in [t_1,t_2] \}, \\ \Psi^{\mathrm{unk}} = \{ & R \geqslant \mathbf{0}_s \,|\, x^{\min} < S(t,x_0,P^{\mathrm{nom}}) + V(t,\mathbf{1}_n)K^{\mathrm{unk}}(t) \\ & < x^{\max},\ \forall K^{\mathrm{unk}} \in \mathbf{P}(R),\ \forall t \in [t_1,t_2] \}. \end{aligned} \tag{14}$$

Checking whether a disturbance amplitude belongs to either of these two sets is impractical because of the need to check for all possible values in $\mathbf{Z}(\alpha)$ or $\mathbf{P}(R)$, respectively. The following result shows that these checks can be made as simple as that for case (a).

Lemma 4.1. *(Transformation of the transient-state tolerableness set). The following statements hold.*

(i) $K^{\mathrm{par}} \in \Psi^{\mathrm{par}}$ *if and only if, for all* $t \in [t_1,t_2]$,

$$S(t,x_0,P^{nom}) + V(t,\zeta^{nom})K^{\mathrm{par}} + W(t)\,\mathrm{diag}\,(\alpha)\,|K^{\mathrm{par}}| < x^{\max}, \tag{15a}$$

$$S(t,x_0,P^{nom}) + V(t,\zeta^{nom})K^{\mathrm{par}} - W(t)\,\mathrm{diag}\,(\alpha)\,|K^{\mathrm{par}}| > x^{\min}, \tag{15b}$$

where

$$W(t) \triangleq \int_0^t |Q(t-\tau)|d\tau \in \mathbb{R}^{(m+n)\times s}, \tag{16a}$$

$$Q(\bar{t}) \triangleq e^{A\bar{t}} \begin{bmatrix} \mathbf{0}_{m\times s} \\ M^{-1}B \end{bmatrix} \in \mathbb{R}^{(m+n)\times s}. \tag{16b}$$

(ii) $R \geqslant \mathbf{0}_s \in \Psi^{\mathrm{unk}}$ *if and only if, for all* $t \in [t_1,t_2]$,

$$S(t,x_0,P^{nom}) + W(t)R < x^{\max}, \tag{17a}$$

$$S(t,x_0,P^{nom}) - W(t)R > x^{\min}. \tag{17b}$$

Proof. We only provide the proof of case *(i)*. The proof of *(ii)* follows similarly.

$\Leftarrow$) Assume K^{par} satisfies (15). Notice that $\forall \zeta^{\mathrm{err}} \in \mathbf{Z}(\alpha)$, $\forall i \in [1,m+n]_{\mathbb{N}}$, it holds that

$$\begin{aligned} [W(t)\,\mathrm{diag}\,(\alpha)\,|K^{\mathrm{par}}|]_i &= \int_0^t |[Q(t-\tau)]_i|\,\mathrm{diag}\,(\alpha)\,|K^{\mathrm{par}}|\mathrm{d}\tau \\ &= \int_0^t \sum_{j=1}^{s} |[Q(t-\tau)]_{i,j}|\alpha_j|K_j^{\mathrm{par}}|\mathrm{d}\tau \\ &\geqslant \int_0^t \sum_{j=1}^{s} [Q(t-\tau)]_{i,j}\zeta_j^{\mathrm{err}}(\tau)K_j^{\mathrm{par}}\mathrm{d}\tau \\ &= \int_0^t [Q(t-\tau)]_i\,\mathrm{diag}\,(\zeta^{\mathrm{err}}(\tau))\,K^{\mathrm{par}}\mathrm{d}\tau \\ &= [V(t,\zeta^{\mathrm{err}})K^{\mathrm{par}}]_i. \end{aligned}$$

Therefore, one has that if (15) holds $\forall t \in [t_1,t_2]$, then the following inequalities hold $\forall t \in [t_1,t_2]$, $\forall \zeta^{\mathrm{err}} \in \mathbf{Z}(\alpha)$,

$$S(t,P^{\mathrm{nom}}) + V(t,\zeta^{\mathrm{nom}})K^{\mathrm{par}} + V(t,\zeta^{\mathrm{err}})K^{\mathrm{par}} < x^{\max}, \tag{18a}$$

$$S(t,P^{\mathrm{nom}}) + V(t,\zeta^{\mathrm{nom}})K^{\mathrm{par}} - V(t,\zeta^{\mathrm{err}})K^{\mathrm{par}} > x^{\min}, \tag{18b}$$

and hence $K^{\mathrm{par}} \in \Psi^{\mathrm{par}}$.

$\Rightarrow$) On the other hand, if $K^{\mathrm{par}} \in \Psi^{\mathrm{par}}$, then (18) holds $\forall t \in [t_1,t_2]$, $\forall \zeta^{\mathrm{err}} \in \mathbf{Z}(\alpha)$. To prove (15), let us show that for all $l \in [1,m+n]_{\mathbb{N}}$, one has

$$[S(t,P^{\mathrm{nom}}) + V(t,\zeta^{\mathrm{nom}})K^{\mathrm{par}} + W(t)\,\mathrm{diag}\,(\alpha)\,|K^{\mathrm{par}}|]_l < x_l^{\max}, \tag{19a}$$

$$[S(t,P^{\mathrm{nom}}) + V(t,\zeta^{\mathrm{nom}})K^{\mathrm{par}} - W(t)\,\mathrm{diag}\,(\alpha)\,|K^{\mathrm{par}}|]_l > x_l^{\min}. \tag{19b}$$

For any $l \in [1,m+n]_{\mathbb{N}}$, we select $\hat{\zeta}^{\mathrm{err}}(t) \in \mathbf{Z}(\alpha)$ as follows: for any $\bar{t} \in [t_1,t_2]$, let

$$\hat{\zeta}_j^{\mathrm{err}}(\tau) = \alpha_l \mathrm{sgn}\{[(Q(\bar{t}-\tau)]_{l,j}K_j^{\mathrm{par}}\},\ \forall j \in [1,s]_{\mathbb{N}}. \tag{20}$$

One can check that $[W(\bar{t})\,\mathrm{diag}\,(\alpha)\,|K^{\mathrm{par}}|]_l = [V(\bar{t},\hat{\zeta}^{\mathrm{err}})K^{\mathrm{par}}]_l$. Therefore, since the lth row of (18a) (resp. (18b)) holds at $t = \bar{t}$, one has that (19a) (resp. (19b)) holds at $t = \bar{t}$. The result follows from the arbitrariness of l and $\bar{t}$. □

Given (13) and Lemma 4.1, it is clear that all the transient-state tolerableness sets Ψ^{pre}, Ψ^{par} and Ψ^{unk} admit a common representation involving certain vector signal (different in each case) being upper and lower bounded over the time interval of interest.

Remark 4.2. *(Containment relations among $\Psi^{\rm pre}$, $\Psi^{\rm par}$ and $\Psi^{\rm unk}$).* The transient-state tolerableness sets for the different types of disturbances are related as follows:

(i) If $|\zeta^{\rm pre}-\zeta^{\rm nom}|$ is upper bounded by α, then $\Psi^{\rm par}\subseteq\Psi^{\rm pre}$;
(ii) If $|\zeta^{\rm pre}|$ is upper bounded by $\mathbb{R}^s\ni\beta^{\rm pre}>0$, then for every $R\in\Psi^{\rm unk}$, it holds $\bar{R}\in\Psi^{\rm pre}$ for all $|\bar{R}|\leqslant \mathrm{diag}(\beta^{\rm pre})^{-1}R$. In particular, if $\beta^{\rm pre}\leqslant\mathbf{1}_s$, then $\Psi^{\rm unk}\subseteq\Psi^{\rm pre}$;
(iii) If $|\zeta^{\rm nom}|$ is upper bounded by $\beta^{\rm nom}\in\mathbb{R}^s$ with $\beta^{\rm nom}+\alpha>0$, then for every $R\in\Psi^{\rm unk}$, it holds that $\bar{R}\in\Psi^{\rm par}$ for all $|\bar{R}|\leqslant (\mathrm{diag}(\beta^{\rm nom}+\alpha))^{-1}R$. In particular, if $\beta^{\rm nom}+\alpha\leqslant\mathbf{1}_s$, then $\Psi^{\rm unk}\subseteq\Psi^{\rm par}$.

These statements follow from Lemma 4.1 by noting that if $|\zeta|$ is upper bounded by $\beta>\mathbf{0}_s$, then $W(t)\,\mathrm{diag}\,(\beta)\geqslant V(t,\zeta)$, for all $t\in[t_1,t_2]$. •

Remark 4.3. *(Extension to linearly coupled safety criteria).* The expressions obtained above for the computation of the transient-state tolerableness sets can be extended to the case where the safety requirements involve linearly coupled states of the form

$$\bar{x}^{\min}<Cx(t)<\bar{x}^{\max},\ \forall t\in[t_1,t_2], \tag{21}$$

where $C\in\mathbb{R}^{c\times(m+n)}$, $\bar{x}^{\max}$, $\bar{x}^{\min}\in\mathbb{R}^c$. A particular example of this scenario is the use of the center of inertia (COI) frequency [32], [33],

$$\omega_{\rm COI}(t)\triangleq\left(\sum_{i=1}^n M_i\omega_i(t)\right)/\sum_{i=1}^n M_i,$$

which corresponds to $C=[M_1,M_2,\cdots,M_n,\mathbf{0}_m^T]/\sum_{i=1}^n M_i$. When the safety criteria is given by (21), the expression (13) to compute $\Psi^{\rm pre}$ should be modified by replacing $S(t,x_0,P^{\rm nom})$ and $V(t,\zeta^{\rm pre})$ by $CS(t,x_0,P^{\rm nom})$ and $CV(t,\zeta^{\rm pre})$, respectively. Similarly, the results in Lemma 4.1 to compute $\Psi^{\rm par}$ and $\Psi^{\rm unk}$ are stil valid by replacing $S(t,x_0,P^{\rm nom})$, $V(t,\zeta^{\rm nom})$ and $W(t)$ by $CS(t,x_0,P^{\rm nom})$, $CV(t,\zeta^{\rm nom})$ and $\int_0^t|CQ(t-\tau)|\mathrm{d}\tau$, respectively. In all cases, $x^{\min}$ (resp. $x^{\max}$) should be replaced by $\bar{x}^{\min}$ (resp. $\bar{x}^{\max}$). •

Remark 4.4. *(Initial state as another disturbance).* In the definitions of tolerableness sets, we assume the initial state x_0 is arbitrary but known. We can also consider the initial condition as another type of disturbance, and characterize the tolerableness sets with respect to both x_0 and $K^{\rm pre}$, $K^{\rm par}$ or R. For instance, consider the definition of $\Psi^{\rm par}$ as

$$\tilde{\Psi}^{\rm par}\triangleq\Big\{(x_0^{\rm est},K^{\rm par})\ \Big|\ \forall\zeta^{\rm err}\in\mathbf{Z}(\alpha),\ \forall x_0\text{ s.t. }|x_0-x_0^{\rm est}|\leqslant x_0^{\rm bnd},\\ \text{(i)-(ii) hold for (2) under (3) and (6)}\Big\},$$

where $x_0^{\rm bnd}\geqslant\mathbf{0}_{m+n}$ constrains the initial state uncertainty. Note that $(x_0^{\rm est},K^{\rm par})\in\tilde{\Psi}^{\rm par}$ means that $K^{\rm par}$ corresponds to a tolerable disturbance for any initial state in a $x_0^{\rm bnd}$-neighborhood around $x_0^{\rm est}$. Similarly to Lemma 4.1, one can show that $(x_0^{\rm est},K^{\rm par})\in\tilde{\Psi}^{\rm par}$ if and only if, for all $t\in[t_1,t_2]$,

$$\begin{aligned}&S(t,x_0^{\rm est},P^{\rm nom})+|e^{At}|x_0^{\rm bnd}+V(t,\zeta^{\rm nom})K^{\rm par}\\ &\qquad+W(t)\,\mathrm{diag}\,(\alpha)\,|K^{\rm par}|<x^{\max},\\ &S(t,x_0^{\rm est},P^{\rm nom})-|e^{At}|x_0^{\rm bnd}+V(t,\zeta^{\rm nom})K^{\rm par}\\ &\qquad-W(t)\,\mathrm{diag}\,(\alpha)\,|K^{\rm par}|>x^{\min}.\end{aligned}$$

For brevity, throughout the rest of the paper, we carry out the exposition for the simpler definition of tolerableness set where the initial condition is not an argument, but the results can be extended accordingly. •

Remark 4.5. *(Tolerableness sets with zero inertia buses).* The equivalent characterization of the tolerableness sets relies on the fact that M is invertible. If this is not the case, one can derive a similar equivalent transformation. For instance, if the disturbance trajectory form is precisely known, the time-domain solution for system (2) under (3) and (4) still takes a linear form with respect to $K^{\rm pre}$, denoted by $x(t)=\hat{S}(t,x_0,P^{\rm nom})+\hat{V}(t,\zeta^{\rm pre})K^{\rm pre}$, and hence one has

$$\begin{aligned}\Psi^{\rm pre}=\Big\{K^{\rm pre}\ \Big|\ &x^{\min}<\hat{S}(t,x_0,P^{\rm nom})\\ &+\hat{V}(t,\zeta^{\rm pre})K^{\rm pre}<x^{\max},\ \forall t\in[t_1,t_2]\Big\}.\end{aligned}$$

Due to the non-zero inertias, $\hat{S}(t,x_0,P^{\rm nom})$, $\hat{V}(t,\zeta^{\rm pre})$ have more complicated expressions than $S(t,x_0,P^{\rm nom})$, $V(t,\zeta^{\rm pre})$), but the ensuing discussion is equally applicable. •

5 Inner and Outer Approximations of the Transient-State Tolerableness Sets

The descriptions of the transient-state tolerableness sets obtained in Section 4 involve infinitely many constraints to check whether a disturbance is tolerable due to the dependence on continuous time. To address this issue, here we construct inner and outer approximations of these sets that are easier to compute and have tunable accuracy. For simplify of exposition, we first consider the case of scalar signals, and then build on this treatment to deal with the vector case.

5.1 Scalar-signal case

Here we deal with the case when the signal that must stay within given upper and lower bounds is scalar. Our discussion here can be interpreted as looking at one component of the actual vector signal. Let $y:\mathbb{R}\times\mathbb{R}^s\to\mathbb{R}$ be a generic scalar signal and let $y^{\min},y^{\max}\in\mathbb{R}$ with $y^{\min}<y^{\max}$. We make the following assumption.

Assumption 5.1. *(Signal differentiability and upper bound).* The signal y is differentiable with respect to its first argument and its derivative is upper bounded by a time-continuous signal uniformly in K, i.e., there exists $y_d:\mathbb{R}\to\mathbb{R}_{\geqslant}$ such that

$$|\dot{y}(t,K)|\leqslant y_d(t),\ \forall t\in[t_1,t_2].$$ •

Consider the set $\Sigma\triangleq\big\{K\ \big|\ y^{\min}<y(t,K)<y^{\max},\ \forall t\in[t_1,t_2]\big\}$. Let us first define a sampling sequence

$$\tau\triangleq\{\tau_1,\tau_2,\dots\tau_r\}, \tag{22}$$

where $r\geqslant 3$ and τ_i's are called sampling points ordered as $t_1=\tau_1<\tau_2<\ldots<\tau_r=t_2$. Our approximations of the set Σ are based on the idea of requiring the signal to be upper and lower bounded at every sampling point, instead of at every time, and making sure that the constraints defining Σ are not violated at all the other times.

The next result makes our approximation methodology precise.

Lemma 5.2. *(Sufficient condition for checking constraints on continuous-time signal). Consider a sampling sequence defined in* (22)*. For each $q\in[1,r-1]_{\mathbb{N}}$, Under Assumption 5.1, define*

$$d_q^\tau\triangleq\max_{t\in[\tau_q,\tau_{q+1}]}\{y_d(t)\}\in\mathbb{R}_{\geqslant}, \tag{23a}$$

$$\delta_q^\tau\triangleq d_q^\tau(\tau_{q+1}-\tau_q)/2\in\mathbb{R}_{\geqslant}. \tag{23b}$$

If

$$y^{\min} + \delta_q^\tau < y(\tau_q, K) \quad < y^{\max} - \delta_q^\tau, \tag{24a}$$
$$y^{\min} + \delta_q^\tau < y(\tau_{q+1}, K) < y^{\max} - \delta_q^\tau, \tag{24b}$$

for all $q \in [1, r-1]_{\mathbb{N}}$*, then* $y^{\min} < y(t,K) < y^{\max}$ *for all* $t \in [t_1, t_2]$.

Proof. We prove that the two upper bounds in (24) imply $y(t,K) < y^{\max}$ for all $t \in [t_1, t_2]$ (the statement for the lower bound follows similarly). For $q \in [1, r-1]_{\mathbb{N}}$, let

$$a \triangleq \frac{y(\tau_q, K) + y(\tau_{q+1}, K)}{2} + \delta_q^\tau.$$

Note that, using (24), one has that $a < y^{\max}$. Let us show that

$$\max_{t \in [\tau_q, \tau_{q+1}]} y(t,K) \leqslant a. \tag{25}$$

It is easy to see that d_q^τ is a Lipschitz constant for y constrained on $[\tau_q, \tau_{q+1}]$. First, we show that $a - y(\tau_q, K) \geqslant 0$ and $a - y(\tau_{q+1}, K) \geqslant 0$. These facts are a consequence of

$$a - y(\tau_q, K) = \frac{1}{2}\big(y(\tau_{q+1}, K) - y(\tau_q, K) + d_q^\tau(\tau_{q+1} - \tau_q)\big),$$
$$a - y(\tau_{q+1}, K) = \frac{1}{2}\big(y(\tau_q, K) - y(\tau_{q+1}, K) + d_q^\tau(\tau_{q+1} - \tau_q)\big),$$

and the fact that $|y(\tau_{q+1}, K) - y(\tau_q, K)| \leqslant d_q^\tau(\tau_{q+1} - \tau_q)$. Next, using the Lipschitz condition, one sees that, if y reaches at some time a starting from the value $y(\tau_q, K)$, it takes at least $(a - y(\tau_q, K))/d_q^\tau > 0$ seconds from τ_q to do so. On the other hand, to come down from such a value, it would take at least $\big(a - y(\tau_{q+1}, K)\big)/d_q^\tau > 0$ seconds, so the total time would be at least $\big(2a - y(\tau_q, K) - y(\tau_{q+1}, K)\big)/d_q^\tau = \tau_{q+1} - \tau_q$. Therefore y cannot reach any value larger than a, i.e., (25) follows, concluding the proof. □

Lemma 5.2 opens the way to efficiently compute inner and outer approximations of the set Σ. The next result formally states this and shows that the two approximations can be made arbitrarily accurate.

Lemma 5.3. *(Inclusion relations and convergence of inner and outer sets). Let* $K \in \mathbb{R}^s$*, and* $t \mapsto y(t,K)$ *satisfy Assumption 5.1. For a sampling sequence* τ*, let*

$$\varepsilon^\tau \triangleq \max_{q \in [1, r-1]_{\mathbb{N}}} \{\tau_{q+1} - \tau_q\} \in \mathbb{R}_>$$

denote its maximum inter-time separation. With the notation of Lemma 5.2, define

$$\Sigma_O^\tau \triangleq \Big\{K \;\Big|\; y^{\min} \leqslant y(\tau_q, K) \leqslant y^{\max}, \quad \forall q \in [1, r]_{\mathbb{N}}\Big\},$$
$$\Sigma_I^\tau \triangleq \Big\{K \;\Big|\; y^{\min} + \delta_q^\tau < y(\tau_q, K),\ y(\tau_{q+1}, K) < y^{\max} - \delta_q^\tau, \quad \forall q \in [1, r-1]_{\mathbb{N}}\Big\}.$$

Then, the following statements hold

(i) $\Sigma_I^\tau \subseteq \Sigma \subseteq \Sigma_{cl} \subseteq \Sigma_O^\tau$*, and*

(ii) for a sequence of sampling sequences $\{\tau(k)\}_{k=1}^\infty$*, if* $\varepsilon^{\tau(k)} \to 0^+$ *as* $k \to \infty$*, then* $\Sigma_O^{\tau(k)} \to \Sigma_{cl}$ *and* $\Sigma_I^{\tau(k)} \to \Sigma$.

Proof. We first prove (i). Since the constraints defining Σ_O^τ all appear in $\Sigma_{\rm cl}$, we deduce $\Sigma_{\rm cl} \subseteq \Sigma_O^\tau$. By Lemma 5.2, it holds that $\Sigma_I^\tau \subseteq \Sigma$.

Next we prove (ii). For each sampling sequence $\tau(k)$, let $\delta^{\max}(k) \triangleq \varepsilon^{\tau(k)} \max_{q \in [1, r(k)-1]_{\mathbb{N}}} d_q^{\tau(k)}/2$. Since $d_q^{\tau(k)}$ is a Lipschitz constant for y constrained on $[\tau_q(k), \tau_{q+1}(k)]$, we have that for all $k \in \mathbb{N}$, $t \in [\tau_q(k), \tau_{q+1}(k)]$ and $q \in [1, r(k)-1]_{\mathbb{N}}$,

$$\begin{aligned}|y(t,K) - y(\tau_q(k), K)| &\leqslant d_q^{\tau(k)}(t - \tau_q(k)) \\ &\leqslant d_q^{\tau(k)}(\tau_{q+1}(k) - \tau_q(k)) = 2\delta_q^{\tau(k)} \leqslant 2\delta^{\max}(k).\end{aligned} \tag{27}$$

Now if $y^{\min} \leqslant y(\tau_1(k), K), \ldots, y(\tau_{r(k)}(k), K) \leqslant y^{\max}$, then by the above inequality one has $y^{\min} - 2\delta^{\max}(k) \leqslant y(t,K) \leqslant y^{\max} + 2\delta^{\max}(k)$ for any $t \in [t_1, t_2]$. Let

$$\hat\Sigma_O^{\tau(k)} \triangleq \Big\{K \;\Big|\; y^{\min} - 2\delta^{\max}(k) \leqslant y(t,K) \leqslant y^{\max} + 2\delta^{\max}(k),\ \forall t \in [t_1, t_2]\Big\}.$$

The above reasoning shows that $\Sigma_O \subseteq \hat\Sigma_O^{\tau(k)}$. Together with (i), we have $\Sigma_{\rm cl} \subseteq \Sigma_O^{\tau(k)} \subseteq \hat\Sigma_O^{\tau(k)}$. Next we show that

$$\hat\Sigma_O^{\tau(k)} \to \Sigma_{\rm cl} \text{ as } k \to \infty, \tag{28}$$

which, by the properties of set limits presented in the preliminaries, suffices to guarantee that $\Sigma_O^{\tau(k)} \to \Sigma_{\rm cl}$ as $k \to \infty$.

To prove (28), we first show that $\limsup_{k\to\infty} \hat\Sigma_O^{\tau(k)} = \Sigma_{\rm cl}$ by pointing out that the two sets mutually contain each other. Since $\Sigma_{\rm cl} \subseteq \hat\Sigma_O^{\tau(j)}$ for every $j \in \mathbb{N}$, it holds that $\Sigma_{\rm cl} \subseteq \bigcup_{j \geqslant k} \hat\Sigma_O^{\tau(j)}$ for every $k \in \mathbb{N}$, which further implies that $\Sigma_{\rm cl} \subseteq \bigcap_{k \geqslant 1} \bigcup_{j \geqslant k} \hat\Sigma_O^{\tau(j)} = \limsup_{k\to\infty} \hat\Sigma_O^{\tau(k)}$. On the other hand, suppose that $K \notin \Sigma_{\rm cl}$, then by the definition of $\Sigma_{\rm cl}$, there exists $\bar t \in [t_1, t_2]$ such that $y(\bar t, K) > y^{\max}$ or $y(\bar t, K) < y^{\min}$. Since by the assumptions, if $j \to \infty$, then $\varepsilon^{\tau(j)} \to 0^+$, which implies that $\delta^{\max}(j) \to 0^+$, one has that $K \notin \hat\Sigma_O^{\tau(j)}$ for every j large enough, i.e., $K \notin \bigcup_{j \geqslant k} \hat\Sigma_O^{\tau(j)}$ for k large enough. This further implies that $K \notin \bigcap_{k \geqslant 1} \bigcup_{j \geqslant k} \hat\Sigma_O^{\tau(j)}$, i.e., $K \notin \limsup_{k\to\infty} \hat\Sigma_O^{\tau(j)}$. Therefore, by contradiction, it holds that $\limsup_{k\to\infty} \hat\Sigma_O^{\tau(k)} \subseteq \Sigma_{\rm cl}$.

Next we show that $\liminf_{k\to\infty} \hat\Sigma_O^{\tau(k)} = \Sigma_{\rm cl}$. Since $\liminf_{k\to\infty} \hat\Sigma_O^{\tau(k)} \subseteq \limsup_{k\to\infty} \hat\Sigma_O^{\tau(k)}$ and we have already proven that $\limsup_{k\to\infty} \hat\Sigma_O^{\tau(k)} = \hat\Sigma_{\rm cl}$, we only need to show that $\hat\Sigma_{\rm cl} \subseteq \liminf_{k\to\infty} \hat\Sigma_O^{\tau(k)}$. This containment holds by noticing that $\hat\Sigma_{\rm cl} \subseteq \hat\Sigma_O^{\tau(j)}$ for every $j \in \mathbb{N}$, which implies that $\hat\Sigma_{\rm cl} \subseteq \bigcup_{k \geqslant 1} \bigcap_{j \geqslant k} \Sigma_O^{\tau(j)} = \liminf_{k\to\infty} \hat\Sigma_O^{\tau(k)}$.

Similarly, by letting

$$\hat\Sigma_I^{\tau(k)} \triangleq \Big\{K \;\Big|\; y^{\min} + \delta^{\max}(k) < y(t,K) < y^{\max} - \delta^{\max}(k),\ \forall t \in [t_1, t_2]\Big\},$$

One has that $\hat\Sigma_I^{\tau(k)} \subseteq \Sigma_I^{\tau(k)} \subseteq \Sigma$ and $\hat\Sigma_I^{\tau(k)} \to \Sigma$ as $k \to \infty$; therefore $\Sigma_I^{\tau(k)} \to \Sigma$ as $k \to \infty$. □

As stated in Lemma 5.3, the inner and outer approximations can be made arbitrarily accurate as ε^τ decreases, at the cost of increasing the cardinality of the sampling sequence, which linearly raises the number of constraints in the definition of the approximations.

5.2 Vector-signal case

Here we build on the treatment of the generic scalar-signal case to construct inner and outer approximations of the transient-state

tolerableness sets $\Psi^{\rm pre}$, $\Psi^{\rm par}$ and $\Psi^{\rm unk}$. In the precisely known case, for every $i \in [1, m+n]_{\mathbb{N}}$, if we let

$$\Psi_i^{\rm pre} \triangleq \Big\{ K^{\rm pre} \;\big|\; x_i^{\min} \leqslant [S(t,x_0,P^{\rm nom})]_i + [V(t,\zeta^{\rm pre})]_i K^{\rm pre} \leqslant x_i^{\max},\ \forall t \in [t_1,t_2] \Big\}, \tag{29}$$

then $\Psi^{\rm pre} = \bigcap_{i\in[1,m+n]_{\mathbb{N}}} \Psi_i^{\rm pre}$. The inner (resp. outer) approximation of each $\Psi_i^{\rm pre}$ follows from Lemma 5.3 with respect to the signal $y(t,K^{\rm pre}) = [S(t,x_0,P^{\rm nom})]_i + [V(t,\zeta^{\rm pre})]_i K^{\rm pre}$ and bounds $y^{\max} = x_i^{\max}$ and $y^{\min} = x_i^{\min}$. Then, the inner (resp. outer) approximation of $\Psi^{\rm pre}$ is just the intersection of inner (resp. outer) approximations for every i. We can also approximate $\Psi^{\rm par}$ and $\Psi^{\rm unk}$ in a similar fashion.

The main difficulty then in applying the scalar-signal results lies in the fact that the signals are not necessarily known a priori, but instead are the result of the effect of the disturbances on the power network dynamics (2). The next result shows that, nevertheless, we can guarantee that Assumption 5.1 is satisfied.

Lemma 5.4. *(Component-wise derivative bound signal). Suppose the amplitude vector $K^{\rm pre}$ (resp. $K^{\rm par}$) in $\Psi^{\rm pre}$ (resp. $\Psi^{\rm par}$), and the magnitude vector R in $\Psi^{\rm unk}$ are bounded as follows,*

$$\|K^{\rm pre}\|_\infty \leqslant \gamma^{\rm pre},\ \|K^{\rm par}\|_\infty \leqslant \gamma^{\rm par},\ \|R\|_\infty \leqslant \gamma^{\rm unk}. \tag{30}$$

For every $i \in [1,n+m]_{\mathbb{N}}$, define

$$z_i^{\rm pre}(t) \triangleq |[S'(t,x_0,P^{nom})]_i| + \gamma^{\rm pre}\|[V'(t,\zeta^{\rm pre})]_i\|_1, \tag{31a}$$

$$z_i^{\rm par}(t) \triangleq |[S'(t,x_0,P^{nom})]_i| + \gamma^{\rm par}\left(\|[V'(t,\zeta^{nom})]_i\|_1 + \alpha_i\|[W'(t)_i\|_1\right), \tag{31b}$$

$$z_i^{\rm unk}(t) \triangleq |[S'(t,x_0,P^{nom})]_i| + \gamma^{\rm unk}\|[W'(t)]_i\|_1, \tag{31c}$$

where $S'(t,x_0,P^{nom})$, $V'(t,\xi)$ and $W'(t)$ are the component-wise time-derivative of $S(t,x_0,P^{nom})$, $V(t,\xi)$ and $W(t)$, and admit the following form

$$S'(t,x_0,P^{nom}) = AS(t,x_0,P^{nom}) + \begin{bmatrix} \mathbf{0}_m \\ M^{-1}P^{nom}(t) \end{bmatrix}, \tag{32a}$$

$$V'(t,\zeta) = AV(t,\zeta) + \begin{bmatrix} \mathbf{0}_{m\times s} \\ M^{-1}B\,\mathrm{diag}\,(\zeta(t)) \end{bmatrix}, \tag{32b}$$

$$W'(t) = |Q(t)|. \tag{32c}$$

Then it holds that for all $i \in [1,m+n]_{\mathbb{N}}$ and for all $t \in [t_1,t_2]$,

$$\frac{d}{dt}\left([S(t,x_0,P^{nom})]_i + [V(t,\zeta^{pre})]_i K^{pre}\right) \leqslant z_i^{\rm pre}(t), \tag{33a}$$

$$\frac{d}{dt}\left([S(t,x_0,P^{nom})]_i + [V(t,\zeta^{nom})]_i K^{par}(\pm)W(t)|K^{par}|\right) \leqslant z_i^{\rm par}(t), \tag{33b}$$

$$\frac{d}{dt}\left([S(t,x_0,P^{nom})]_i(\pm)W(t)R\right) \leqslant z_i^{\rm par}(t). \tag{33c}$$

Proof. One can easily verify (32a) and (32b) using the chain rule. For (32c), by letting $\bar\tau = t-\tau$, one has

$$W(t) = \int_0^t |Q(t-\tau)|\mathrm{d}\tau = \int_0^t |Q(\bar\tau)|\mathrm{d}\bar\tau,$$

and hence $W'(t) = |Q(t)|$ follows immediately.

Next, since $\mathrm{d}\left([S(t,x_0,P^{\rm nom})]_i + [V(t,\zeta^{\rm pre})]_i K^{\rm pre}\right)/\mathrm{d}t = [S'(t,x_0,P^{\rm nom})]_i + [V'(t,\zeta^{\rm pre})]_i K^{\rm pre} \leqslant |[S'(t,x_0,P^{\rm nom})]_i| + \|K^{\rm pre}\|_\infty \|[V'(t,\zeta^{\rm pre})]_i\|_1 \leqslant z_i^{\rm pre}(t)$, one has (33a) holds. The rest follows similarly. □

Lemma 5.4 allows us to use the results for generic scalar signals to construct the set approximations in the case of vector signals generated by power network dynamics subject to disturbances.

Theorem 5.5. *(Inclusion relations and convergence of inner and outer sets for the transient-state tolerableness set). For every $i \in [1,n+m]_{\mathbb{N}}$, let $\tau^i = \{\tau_1^i, \tau_2^i, \ldots, \tau_{r(i)}^i\}$ be a sampling sequence and define for each $\lambda \in \{pre, par, unk\}$,*

$$\varepsilon^{\tau^i} \triangleq \max_{q\in[1,r(i)-1]_{\mathbb{N}}} \{\tau_{q+1}^i - \tau_q^i\},$$

$$d_{q,i}^\lambda \triangleq \max_{t\in[\tau_q^i,\tau_{q+1}^i]} \{z_i^\lambda(t)\},\ \forall q \in [1,r(i)-1]_{\mathbb{N}},$$

$$\delta_{q,i}^\lambda \triangleq d_{q,i}^\lambda(\tau_{q+1}^i - \tau_q^i)/2,\ \forall q \in [1,r(i)-1]_{\mathbb{N}}.$$

Given the sets defined in (34)*, let*

$$\Psi_O^{pre} \triangleq \bigcap_{i\in[1,n+m]_{\mathbb{N}}} \Psi_{O,i}^{pre}, \tag{35a}$$

$$\Psi_I^{pre} \triangleq \bigcap_{i\in[1,n+m]_{\mathbb{N}}} \Psi_{I,i}^{pre}, \tag{35b}$$

$$\Psi_O^{par} \triangleq \bigcap_{i\in[1,n+m]_{\mathbb{N}}} (\overline{\Psi}_{O,i}^{par} \cap \underline{\Psi}_{O,i}^{par}), \tag{35c}$$

$$\Psi_I^{par} \triangleq \bigcap_{i\in[1,n+m]_{\mathbb{N}}} (\overline{\Psi}_{I,i}^{par} \cap \underline{\Psi}_{I,i}^{par}), \tag{35d}$$

$$\Psi_O^{unk} \triangleq \bigcap_{i\in[1,n+m]_{\mathbb{N}}} (\overline{\Psi}_{O,i}^{unk} \cap \underline{\Psi}_{O,i}^{unk}), \tag{35e}$$

$$\Psi_I^{unk} \triangleq \bigcap_{i\in[1,n+m]_{\mathbb{N}}} (\overline{\Psi}_{I,i}^{unk} \cap \underline{\Psi}_{I,i}^{unk}). \tag{35f}$$

Then, the following statements hold for any $\lambda \in \{\rm pre, par, unk\}$,

(i) $\Psi_I^\lambda \subseteq \Psi^\lambda \subseteq \Psi_{cl}^\lambda \subseteq \Psi_O^\lambda$*, and*

(ii) if $\varepsilon^{\tau^i} \to 0^+$ for all $i \in [1,m+n]_{\mathbb{N}}$, then $\Psi_O^\lambda \to \Psi_{cl}^\lambda$ and $\Psi_I^\lambda \to \Psi^\lambda$.

Proof. We only prove the case $\lambda = $ pre (the other two cases follow similarly). Notice that each $\Psi_i^{\rm pre}$ defined in (29) can be approximated individually using Lemma 5.3 by letting $y(t,K^{\rm pre}) = [S(t,x_0,P^{\rm nom})]_i + [V(t,\zeta^{\rm pre})]_i K^{\rm pre}$. The corresponding time-derivative bound signal is $y_d = z_i^{\rm pre}$, which follows from Lemma 5.4. Therefore, it holds that for every $i \in [1,m+n]_{\mathbb{N}}$, $\Psi_{I,i}^{\rm pre} \subseteq \Psi_i^{\rm pre} \subseteq \Psi_{i,\rm cl}^{\rm pre} \subseteq \Psi_{O,i}^{\rm pre}$, and $\Psi_{O,i}^{\rm pre} \to \Psi_{\rm cl}^{\rm pre}$ and $\Psi_I^\lambda \to \Psi^{\rm pre}$ as $\varepsilon^{\tau^i} \to 0^+$. Since finite intersections preserve containment relations and set limits, statements (i) and (ii) follow. □

Even though we assume for simplicity that the time interval $[t_1,t_2]$ is the same for each component of $x(t)$, note that this can be easily extended to scenarios where each $x_i(t)$ has its own time sampling interval $[t_1^i, t_2^i]$.

Remark 5.6. *(Bound on the disturbance amplitude).* Theorem 5.5 requires an a priori bound on the norm of $K^{\rm pre}$ (resp. $K^{\rm par}$ and R) to obtain the set $\Psi_I^{\rm pre}$ (resp. $\Psi_I^{\rm par}$ and $\Psi_I^{\rm unk}$). This assumption is reasonable in the sense that the energy of the disturbance should be upper bounded. Alternatively, since $\Psi_O^{\rm pre}$ (resp. $\Psi_O^{\rm par}$ and $\Psi_O^{\rm unk}$) can be computed without any knowledge of the norm bound, one can obtain an upper bound on the norm of $K^{\rm pre}$, for instance, by solving $\max_{K\in\Psi_O^{\rm pre}} \|K\|_\infty$, provided that $\Psi_O^{\rm pre}$ is bounded. •

Remark 5.7. *(Computational complexity).* Note that both $\Psi_{\rm I}^\lambda$ and $\Psi_{\rm O}^\lambda$ for any $\lambda \in \{\rm pre, par, unk\}$ consist of only linear constraints, and hence are convex sets, where the number of constraints appearing in them are, depending on the case, either $2\sum_{i=1}^{m+n} r(i)$ or $4\sum_{i=1}^{m+n} r(i)$. This implies that the complexity of characterizing

$$
\begin{aligned}
\Psi^{\text{pre}}_{O,i} &\triangleq \left\{K^{\text{pre}} \;\middle|\; x_i^{\min} \leqslant [S(\tau_q^i,x_0,P^{\text{nom}})]_i + [V(\tau_q^i,\zeta^{\text{pre}})]_i K^{\text{pre}} \leqslant x_i^{\max},\ \forall q \in [1,r(i)]_{\mathbb{N}}\right\},\\
\Psi^{\text{pre}}_{I,i} &\triangleq \left\{K^{\text{pre}} \;\middle|\; x_i^{\min} + \delta^{\text{pre}}_{q,i} < [S(t,x_0,P^{\text{nom}})]_i + [V(t,\zeta^{\text{pre}})]_i K^{\text{pre}} < x_i^{\max} - \delta^{\text{pre}}_{q,i},\ \forall t \in \{\tau_q^i,\tau_q^{i+1}\},\ \forall q \in [1,r(i)-1]_{\mathbb{N}}\right\},\\
\overline{\Psi}^{\text{par}}_{O,i} &\triangleq \left\{K^{\text{par}} \;\middle|\; [S(\tau_q^i,x_0,P^{\text{nom}})]_i + [V(\tau_q^i,\zeta^{\text{nom}})]_i K^{\text{par}} + W(\tau_q^i)|K^{\text{par}}| \leqslant x_i^{\max},\ \forall q \in [1,r(i)]_{\mathbb{N}}\right\},\\
\underline{\Psi}^{\text{par}}_{O,i} &\triangleq \left\{K^{\text{par}} \;\middle|\; [S(\tau_q^i,x_0,P^{\text{nom}})]_i + [V(\tau_q^i,\zeta^{\text{nom}})]_i K^{\text{par}} - W(\tau_q^i)|K^{\text{par}}| \geqslant x_i^{\min},\ \forall q \in [1,r(i)]_{\mathbb{N}}\right\},\\
\overline{\Psi}^{\text{par}}_{I,i} &\triangleq \left\{K^{\text{par}} \;\middle|\; [S(t,x_0,P^{\text{nom}})]_i + [V(t,\zeta^{\text{nom}})]_i K^{\text{par}} + W(t)|K^{\text{par}}| < x_i^{\max} - \delta^{\text{par}}_{q,i},\ \forall t \in \{\tau_q^i,\tau_q^{i+1}\},\ \forall q \in [1,r(i)-1]_{\mathbb{N}}\right\},\\
\underline{\Psi}^{\text{par}}_{I,i} &\triangleq \left\{K^{\text{par}} \;\middle|\; [S(t,x_0,P^{\text{nom}})]_i + [V(t,\zeta^{\text{nom}})]_i K^{\text{par}} - W(t)|K^{\text{par}}| > x_i^{\min} + \delta^{\text{par}}_{q,i},\ \forall t \in \{\tau_q^i,\tau_q^{i+1}\},\ \forall q \in [1,r(i)-1]_{\mathbb{N}}\right\},\\
\overline{\Psi}^{\text{unk}}_{O,i} &\triangleq \left\{R \;\middle|\; [S(\tau_q^i,x_0,P^{\text{nom}})]_i + W(\tau_q^i)R \leqslant x_i^{\max},\ \forall q \in [1,r(i)]_{\mathbb{N}}\right\},\\
\underline{\Psi}^{\text{unk}}_{O,i} &\triangleq \left\{R \;\middle|\; [S(\tau_q^i,x_0,P^{\text{nom}})]_i - W(\tau_q^i)R \geqslant x_i^{\min},\ \forall q \in [1,r(i)]_{\mathbb{N}}\right\},\\
\overline{\Psi}^{\text{unk}}_{I,i} &\triangleq \left\{R \;\middle|\; [S(t,x_0,P^{\text{nom}})]_i + W(t)R < x_i^{\max} - \delta^{\text{unk}}_{q,i},\ \forall t \in \{\tau_q^i,\tau_q^{i+1}\},\ \forall q \in [1,r(i)-1]_{\mathbb{N}}\right\},\\
\underline{\Psi}^{\text{unk}}_{I,i} &\triangleq \left\{R \;\middle|\; [S(t,x_0,P^{\text{nom}})]_i - W(t)R > x_i^{\min} + \delta^{\text{unk}}_{q,i},\ \forall t \in \{\tau_q^i,\tau_q^{i+1}\},\ \forall q \in [1,r(i)-1]_{\mathbb{N}}\right\}.
\end{aligned}
\tag{34}
$$

such sets grows linearly with respect to the number of sampling points, and, if we take the $r(i)$'s equal for each component, then it also grows linearly with $m+n$, i.e., the number of states. Furthermore, the approximations also scale well with the dimension of K because of the linear dependence of the system trajectories on this parameter.

The actual computation of the approximation sets involves the evaluation of several time-varying matrices (e.g., $S(t,x_0,P^{\text{nom}})$, $V(t,\zeta^{\text{pre}})$, $W(t)$, etc.) at each sampling time. Here, we briefly describe the procedure we employ to do this for $S(t,x_0,P^{\text{nom}})$ at $t=\tau_1^i,\tau_2^i,\cdots,\tau_r^i$ for each $i\in[1,n+m]_{\mathbb{N}}$ (other procedures are also possible). Using a first-order approximation, for sufficiently small $T>0$ and any $n\in\mathbb{N}$, we can write

$$
\begin{aligned}
&S((n+1)T,x_0,P^{\text{nom}}) \approx S(nT,x_0,P^{\text{nom}}) + TS'(nT,x_0,P^{\text{nom}})\\
&= S(nT,x_0,P^{\text{nom}}) + TAS(nT,x_0,P^{\text{nom}}) + T\begin{bmatrix}\mathbf{0}_m\\ M^{-1}P^{\text{nom}}(nT)\end{bmatrix},
\end{aligned}
$$

where the equality follows from substituting $S'(nT,x_0,P^{\text{nom}})$ by (32a). Using this equation, one can iteratively compute the value of $S(t,x_0,P^{\text{nom}})$ at $t=0,T,2T,3T,\ldots$. For T much smaller than the distance between consecutive sampling points, one can report to this approximation to evaluate $S(t,x_0,P^{\text{nom}})$ at the sampling points. •

Remark 5.8. *(Robustness metric based on tolerableness set).* One can synthesize metrics that quantify the robustness to disturbances of the power network at a given steady state using the transient-state tolerableness set. The basic idea is to identify the smallest (with respect to some criteria) disturbance that leads to a violation of the safety criteria (i)-(ii). Formally, for $\lambda\in\{\text{pre},\text{par},\text{unk}\}$, one can define the metric, denoted by β^λ, as the optimal value of the following optimization problem,

$$
\begin{aligned}
\inf\quad & f(K) && \text{(36a)}\\
\text{s.t.}\quad & K\notin\Psi^\lambda, && \text{(36b)}\\
& g(K)\leqslant 0, && \text{(36c)}
\end{aligned}
$$

where $f:\mathbb{R}^s\mapsto\mathbb{R}$ is a measurement of the disturbance energy, say, $f(K)=\|K\|_2$, and (36c) represents some other constraints for the disturbance. Since we cannot precisely compute Ψ^λ, one can alternatively compute the optimal value, denoted β_I^λ (resp. β_O^λ), of the following optimization problem

$$
\begin{aligned}
\inf\quad & f(K) && \text{(37a)}\\
\text{s.t.}\quad & K\notin\Psi_O^\lambda(\text{resp. }\Psi_I^\lambda), && \text{(37b)}\\
& g(K)\leqslant 0. && \text{(37c)}
\end{aligned}
$$

By Theorem 5.5, one has that $\beta_I^\lambda\leqslant\beta^\lambda\leqslant\beta_O^\lambda$. If f is continuous, as $\varepsilon^{\tau^i}\to 0^+$ for all $i\in[1,m+n]_{\mathbb{N}}$, it holds that $\beta_I^\lambda\to\beta^\lambda$ and $\beta_O^\lambda\to\beta^\lambda$, i.e., we can upper and lower bound β^λ with an arbitrary degree of accuracy.

Although constraint (37b) is nonconvex (since it corresponds to the complement of a convex polytope), we can decompose (37b) into a finite union of linear constraints. We take $\lambda=$pre as an example. Define for each $q\in[1,r(i)]$,

$$
\begin{aligned}
\Psi^{\text{pre}}_{O,i,q} \triangleq \Big\{K^{pre} \;\Big|\; & x_i^{\min} \leqslant [S(\tau_q^i,x_0,P^{\text{nom}})]_i + [V(\tau_q^i,\zeta^{\text{pre}})]_i K^{\text{pre}}\\
& \leqslant x_i^{\max}\Big\}.
\end{aligned}
$$

Then we deduce $\Psi_O^{\text{pre}}=\bigcap_{i\in[1,m+n]_{\mathbb{N}}}\bigcap_{q\in[1,r(i)]_{\mathbb{N}}}\Psi^{\text{pre}}_{O,i,q}$. Now denote $\beta^{\text{pre}}_{O,i,q}$ as the optimal solution of

$$
\begin{aligned}
\inf\quad & f(K) && \text{(38a)}\\
\text{s.t.}\quad & K\notin\Psi^\lambda_{O,i,q}, && \text{(38b)}\\
& g(K)\leqslant 0. && \text{(38c)}
\end{aligned}
$$

One can see that β_O^{pre} equals the smallest value among $\beta^{\text{pre}}_{O,i,q}$ over all possible i and q. Notice now (38b) is a linear constraint, and if f and g are convex, then (38) is a convex optimization problem. In the same way, we can compute β_I^{pre}. This strategy also works for $\lambda\in\{\text{pre},\text{par}\}$. •

6 Optimizing the Sampling Sequence

A relevant question regarding the inner and outer approximations developed above is how to precisely quantify how well they approximate the corresponding transient-state tolerableness set. With metrics available to provide such quantification, one can then ask the question of how to optimize the location of a fixed number of sampling points in order to provide better approximations. This aim is motivated by the fact that the complexity of characterizing

the approximations grows with the number of constraints defining them. To answer these questions, we first consider the scalar-signal case and quantify the approximation gap between Σ_I^τ (resp. Σ_O^τ) and Σ (resp. $\Sigma_{\rm cl}$). We then propose an provably correct algorithmic procedure to find the optimal sampling sequence and generalize our treatment to the vector-signal case.

6.1 Metric measuring the approximation gap

Here we define a metric to quantify the gap between the inner and outer approximations and the actual set. To do so, we find it useful to introduce the following set definitions with the same functional form as Σ,

$$\bar{\Sigma}_O^\tau \triangleq \Big\{ K \,\Big|\, y^{\min} - 2\delta_q^\tau \leqslant y(t,K) \leqslant y^{\max} + 2\delta_q^\tau,\ \forall t \in [\tau_q, \tau_{q+1}],\ \forall q \in [1, r-1]_{\mathbb{N}} \Big\}, \tag{39a}$$

$$\bar{\Sigma}_I^\tau \triangleq \Big\{ K \,\Big|\, y^{\min} + \delta_q^\tau < y(t,K) < y^{\max} - \delta_q^\tau,\ \forall t \in [\tau_q, \tau_{q+1}],\ \forall q \in [1, r-1]_{\mathbb{N}} \Big\}. \tag{39b}$$

Given the similarity in their definitions with Σ, these sets are easier to compare with it than the original Σ_I^τ and Σ_O^τ. In addition, note that by (27), it holds that $\Sigma_O^\tau \subseteq \bar{\Sigma}_O^\tau$, and since all constraints in Σ_I^τ appear in $\bar{\Sigma}_I^\tau$ as well, one has that $\bar{\Sigma}_I^\tau \subseteq \Sigma_I^\tau$. Therefore a conservative but guaranteed way to describe the approximation is to depict the gap between $\bar{\Sigma}_I^\tau$ and Σ, and between $\Sigma_{\rm cl}$ and $\bar{\Sigma}_O^\tau$.

To quantify the gap between $\bar{\Sigma}_I^\tau$ and Σ, we define the approximation metric as

$$\nu(\tau) \triangleq \max_{q \in [1, r-1]_{\mathbb{N}}} \{\delta_q^\tau\}. \tag{40}$$

The explanation for this choice is as follows. For a given $q \in [1, r-1]_{\mathbb{N}}$, all the K's that satisfy $y^{\min} \leqslant y(t,K) \leqslant y^{\max},\ \forall t \in [\tau_q, \tau_{q+1}]$ while do not satisfy $y^{\min} + \delta_q^\tau \leqslant y(t,K) \leqslant y^{\max} - \delta_q^\tau,\ \forall t \in [\tau_q, \tau_{q+1}]$ are given by $cns(\delta_q^\tau)$ as defined in (41). The region $cns(\delta_q^\tau)$ becomes smaller as δ_q^τ decreases, and is empty if δ_q^τ is 0. Hence a proxy to measure the size of $cns(\delta_q^\tau)$ is simply δ_q^τ. Furthermore, by noting that $\nu(\tau)$ characterizes the largest size of all $cns(\delta_q^\tau)$'s and that $\Sigma \backslash \bar{\Sigma}_I^\tau$ is a subset of $\bigcup_{q \in [1, r-1]_{\mathbb{N}}} cns(\delta_q^\tau)$, we conclude $\nu(\tau)$ measures the gap between $\bar{\Sigma}_I^\tau$ and Σ. Given the symmetry with the definition of $\bar{\Sigma}_O^\tau$, note that one can also use the metric to measure the gap between $\bar{\Sigma}_O^\tau$ and $\Sigma_{\rm cl}$.

Our next result characterizes the minimization of ν. Formally, consider

$$\min_{\tau} \quad \nu(\tau) \tag{42a}$$

$$\text{s.t.} \quad t_1 = \tau_1 < \tau_2 < \ldots < \tau_r = t_2. \tag{42b}$$

This problem possesses a unique global minimizer, which can be equivalently characterized by a set of equations.

Proposition 6.1. *(Characterization of global optimum of metric). The optimization problem* (42) *has a unique global minimizer, which is uniquely determined by,*

$$\delta_i^\tau = \delta_{i+1}^\tau,\ \forall i \in [1, r-2]_{\mathbb{N}}, \tag{43a}$$

$$\tau_1 = t_1,\ \tau_r = t_2. \tag{43b}$$

Proof. Note that the result holds if the following three statements are true:

(i) There exists at least one global minimizer for (42)
(ii) Any global minimizer of (42) satisfies condition (43).
(iii) There exists a unique solution for (43).

To see this, by (i) and (ii), a solution for (43) exists. By (iii), since the solution for (43) is unique, it has to be the only global minimizer. Our strategy is then to prove (i)-(iii) separately.

To prove (i), consider the optimization problem (42) but with non-strict inequality constraints. Since ν is continuous and the constraints define a compact feasibility set, by the extreme value theorem [34], there exists at least one global minimizer $\bar{\tau}^*$. If at least one of these minimizers satisfies the constraint (42b), then it is also a global minimizer of (42). If it does not, then it is easy to find a sampling sequence $\hat{\tau}^*$ that satisfies the constraint and has at most the same metric value. In fact, without loss of generality, assume that $\bar{\tau}_{q-1}^* < \bar{\tau}_q^* = \bar{\tau}_{q+1}^* = \cdots = \bar{\tau}_{q+k}^* < \bar{\tau}_{q+1}^*$ for some $q \in [1, r-1]_{\mathbb{N}}$ and $k \in \mathbb{N}$. Let $\hat{\tau}_j^* = \bar{\tau}_j^*$ for every $j \in [1, r]_{\mathbb{N}} / [q, q+k-1]_{\mathbb{N}}$ and $\hat{\tau}_j^* = \bar{\tau}_{q-1}^* + (\bar{\tau}_q^* - \bar{\tau}_{q-1}^*)(j-q+1)/(k+1)$ for every $j \in [q, q+k-1]_{\mathbb{N}}$. By this way one can easily check that $\nu(\hat{\tau}^*) \leqslant \nu(\bar{\tau}^*)$ holds.

We prove statement (ii) by contradiction. Suppose (42) admits a global minimizer τ that does not satisfy condition (43) and let us construct another sequence $\bar{\tau}$ with $\nu(\bar{\tau}) < \nu(\tau)$. We first consider the case where consecutive subintervals achieve the same maximum value, i.e., for some $k \in \mathbb{N} \cup \{0\}$, it holds that $\delta_j^\tau < \delta_q^\tau = \delta_{q+1}^\tau = \cdots = \delta_{q+k}^\tau = \nu(\tau)$ for every $j \in [1, r-1]_{\mathbb{N}} \backslash [q, q+k]_{\mathbb{N}}$. Since condition (43) does not hold, either $\tau_q \neq t_1$ or $\tau_{q+k} \neq t_2$. Without loss of generality, assume the first case. Now construct $\bar{\tau}$ by letting $\bar{\tau}_j = \tau_j$ for every $j \in [1, r]_{\mathbb{N}} \backslash [q, q+k]_{\mathbb{N}}$ and $\bar{\tau}_j = \tau_j + {\rm d}x_j$ for every $j \in [q, q+k]_{\mathbb{N}}$, where ${\rm d}x_j$ is determined as follows: since every δ_j^τ is a strictly monotonically decreasing and continuous function of τ_j, one can always find ${\rm d}x_j > 0$ small enough for every $j \in [q, q+k]_{\mathbb{N}}$ such that $\delta_{q-1}^{\bar{\tau}} < \delta_j^{\bar{\tau}} < \delta_q^\tau = \delta_{q+1}^\tau = \cdots = \delta_{q+k}^\tau$ holds for every $j \in [q, q+k]_{\mathbb{N}}$, which implies that $\nu(\bar{\tau}) < \nu(\tau)$. In the most general case where there are several groups of consecutive subintervals achieving the same maximum value, and all groups share no common sampling point, one can construct $\bar{\tau}$ by tuning the points using the idea above for each individual group, resulting in $\nu(\bar{\tau}) < \nu(\tau)$.

To prove statement (iii), assume there exist two different sampling sequences τ^a and τ^b that both satisfy condition (43). We first consider the case when $\delta_i^{\tau^a} \neq \delta_i^{\tau^b}$ for every $i \in [1, r-1]_{\mathbb{N}}$, and, without loss of generality, assume that $\delta_i^{\tau^a} < \delta_i^{\tau^b}$. Notice that if $\tau_2^b \leqslant \tau_2^a$, then

$$\begin{aligned} \delta_1^{\tau^b} &\triangleq (\tau_2^b - t_1)/2 \max_{t \in [t_1, \tau_2^b]} \{y_d(t)\} \\ &\leqslant (\tau_2^a - t_1)/2 \max_{t \in [t_1, \tau_2^a]} \{y_d(t)\} = \delta_1^{\tau^a}, \end{aligned}$$

violating the assumption, and hence $\tau_2^b > \tau_2^a$. Similarly, it holds that $\tau_3^b > \tau_3^a$. Along this one has that $\tau_{r-1}^b > \tau_{r-1}^a$. The contradiction occurs as one can easily see that $\delta_{r-1}^{\tau^b} \leqslant (t_2 - \tau_2^a)/2 \max_{t \in [t_1, \tau_2^a]} \{y_d(t)\} = \delta_{r-1}^{\tau^a}$. Next, we consider the case when $\delta_i^{\tau^a} = \delta_i^{\tau^b}$ for every $i \in [1, r-1]_{\mathbb{N}}$. Since δ_1^τ is a strictly monotonically increasing function of τ_2, to have $\delta_1^{\tau_b} = \delta_1^{\tau_b}$, it must hold that $\tau_2^a = \tau_2^b$. Similarly, $\tau_i^a = \tau_i^b$ for every $i \in [1, r]_{\mathbb{N}}$, i.e., τ^a and τ^b are the same sequence. Therefore, equation (43) admits only one solution. □

Given Proposition 6.1, we denote the unique minimizer of (42) by τ^*, and the optimal value by $\nu(\tau^*)$.

6.2 Algorithm to reduce the approximation gap

Here, we introduce a strategy that, for a fixed number r of sampling points, finds the sampling sequence that minimizes v.

$$
\begin{aligned}
cns(\delta_q^\tau) \triangleq & \left\{K \mid y^{\min} < y(t,K) < y^{\max}, \quad \forall t \in [\tau_q, \tau_{q+1}]\right\} \setminus \left\{K \mid y^{\min} + \delta_q^\tau < y(t,K) < y^{\max} - \delta_q^\tau, \quad \forall t \in [\tau_q, \tau_{q+1}]\right\} \\
= & \left(\left\{K \mid y^{\max} - \delta_q^\tau \leqslant y(t,K) < y^{\max}, \quad \forall t \in [\tau_q, \tau_{q+1}]\right\} \bigcap \left\{K \mid y^{\min} < y(t,K), \quad \forall t \in [\tau_q, \tau_{q+1}]\right\}\right) \bigcup \\
& \left(\left\{K \mid y^{\min} < y(t,K) \leqslant y^{\min} + \delta_q^\tau, \quad \forall t \in [\tau_q, \tau_{q+1}]\right\} \bigcap \left\{K \mid y(t,K) < y^{\max}, \quad \forall t \in [\tau_q, \tau_{q+1}]\right\}\right) \qquad (41)
\end{aligned}
$$

Our design is based on Proposition 6.1. Notice that we can equivalently obtain τ^* by solving the transcendental equations (43). Based on this equivalence relation, we propose Algorithm 1 to provide a sampling sequence $\hat{\tau}$ whose metric value $v(\hat{\tau})$ can be made arbitrarily close to $v(\tau^*)$. The algorithm proceeds by approximating $v(\tau^*)$ through the bisection method, i.e., starts from an initial interval that contains $v(\tau^*)$, and iteratively obtains intervals containing $v(\tau^*)$ whose length is half the length of the one generated in the previous step. This process terminates when the approximation is optimal within a prescribed tolerance error.

Algorithm 1: Obtain near-optimal sampling sequence

Data: Derivative bound signal y_d, tolerance error value $v^{\text{err}} > 0$, t_1 and t_2
Result: Near-optimal value η^N and near-optimal sequence $\hat{\tau}$

1 Initialization: $\tau_i^{\text{even}} = t_1 + (i-1)(t_2-t_1)/(r-1)\ \forall i \in [1,r]_{\mathbb{N}}$, $a^0 = 0$, $b^0 = v(\tau^{\text{even}})$, $\eta^0 = (a^0+b^0)/2$, $k = 0$, $flag$=true
2 **while** *flag* **do**
3 $\tau_1^k = t_1$, $\tau_r^k = t_2$
4 **for** $i = 2 : r-1$ **do**
5 Set τ_i^k such that $\delta_{i-1}^{\tau^k} = \eta^k$
6 **end**
7 **if** $b^k - a^k \leqslant v^{error}/2$ **then**
8 $N = k$, $flag$=false
9 **end**
10 Compute $\delta_{r-1}^{\tau^k}$
11 **if** $\delta_{r-1}^{\tau^k} - \eta^k > 0$ **then**
12 $a^{k+1} = \eta^k$, $b^{k+1} = b^k$
13 **else**
14 $a^{k+1} = a^k$, $b^{k+1} = \eta^k$
15 **end**
16 $\eta^{k+1} = (a^{k+1} + b^{k+1})/2$, $k = k+1$
17 **end**
18 $\hat{\tau}_1 = t_1$, $\hat{\tau}_r = t_2$
19 **for** $i = 2 : r-1$ **do**
20 Set $\hat{\tau}_i$ such that $\delta_{i-1}^{\hat{\tau}} = \eta^N + v^{\text{err}}/2$
21 **end**

The following result formally characterizes the convergence properties of Algorithm 1.

Proposition 6.2. *(Algorithm 1 finds optimal sampling sequence). Given a tolerance error $v^{err} > 0$, there exists a unique N such that the sampling sequence τ^k, $k \in [1,N]_{\mathbb{N}}$ and outputs η^N, $\hat{\tau}$ from Algorithm 1 satisfy*

(i) $|\eta^k - v(\tau^*)| \leqslant v(\tau^{even})2^{-k}$ *for every* $k \in [1,N]_{\mathbb{N}}$;
(ii) $|\eta^N - v(\tau^*)| \leqslant v^{err}/2$, *with* $N < \log_2 v(\tau^0) - \log_2 v^{err} + 2$;
(iii) $v(\hat{\tau}) \leqslant v(\tau^*) + v^{err}$.

Proof. With the notation of Algorithm 1, we first show that for the sampling sequence τ^k, if $\delta_{r-1}^{\tau^k} > \eta^k$, then $\eta^k < v(\tau^*)$. One can see that since $\eta^k = \delta_1^{\tau^k} = \delta_2^{\tau^k}, \cdots, = \delta_{r-2}^{\tau^k}$, if $\eta^k \geqslant v(\tau^*)$, then using the same argument as in the proof of Proposition 6.1(ii), it holds that $\tau_i^k \geqslant \tau_i^*$ for any $i \in [2,r-1]_{\mathbb{N}}$, leading to $\delta_{r-1}^{\tau^k} \leqslant \delta_{r-1}^{\tau^*} = v(\tau^*) \leqslant \eta^k$, which contradicts the assumption. Similarly, one can prove that if $\delta_{r-1}^{\tau^k} \leqslant \eta^k$, then $\eta^k \geqslant v(\tau^*)$. Along with these observations, one can easily see that via step 11 to step 16, plus the initialization condition, it holds that $v(\tau^*) \in [a^k, b^k]$ for every $k \in [1,N]_{\mathbb{N}}$, and $b^{k+1} - a^{k+1} = (b^k - a^k)/2$. Finally, statement (i) holds by noticing that $|\eta^k - v(\tau^*)| \leqslant b^k - a^k = (b^0 - a^0)/2^k = v(\tau^0)/2^k$. This implies that $v(\tau^k)$ exponentially converges to the optimal value $v(\tau^*)$.

The first part of statement (ii) is simply due to the termination condition in step 7 in Algorithm 1. Since $k = N$ is the first satisfying $b^k - a^k \leqslant v^{\text{error}}/2$, it holds that $v^{\text{error}}/2 < b^{N-1} - a^{N-1} = v(\tau^0)/2^{N-1}$, and hence the rest of statement (ii) follows immediately.

To prove statement (iii), notice $\delta_i^{\hat{\tau}} = \eta^N + v^{\text{err}}/2 \geqslant v(\tau^*) = \delta_j^{\tau^*}$ for any $i, j \in [1,r-1]_{\mathbb{N}}$, where the inequality follows from (ii). Therefore, $\delta_i^{\hat{\tau}} \geqslant \delta_i^{\tau^*}$ for every $i \in [1,r-1]_{\mathbb{N}}$, which implies that $\hat{\tau}_i \geqslant \tau_i^*$ for every $i \in [1,r-1]_{\mathbb{N}}$, and hence $\delta_{r-1}^{\hat{\tau}} \leqslant \delta_{r-1}^{\tau^*} = v(\tau^*)$. Now, one has

$$
\begin{aligned}
v(\hat{\tau}) &= \max\{\eta^N + v_{\text{err}}/2, \delta_{r-1}^{\hat{\tau}}\} \\
&\leqslant \max\{\eta^N + v_{\text{err}}/2, v(\tau^*)\} = \eta^N + v_{\text{err}}/2 \leqslant v(\tau^*) + v^{\text{err}},
\end{aligned}
$$

where the last inequality follows from (ii). □

Notice that steps 5 and 20 of Algorithm 1 require the solution of a transcendental equation in one variable. Even though an exact solution is not available, we discuss in the following remark a bisection method to approximate it with an arbitrary degree of accuracy.

Remark 6.3. *(Solving transcendental equation in one variable).* Here we describe a strategy to approximate the solution in steps 5 and 20 of Algorithm 1. For conciseness, we describe it in general as Algorithm 2: one can apply it to solve step 5 (resp. step 20) by simply letting $\tau = \tau^k$ (resp. $\tau = \hat{\tau}$) and $\eta = \eta^k$ (resp. $\eta = \eta^N$). Algorithm 2 uses bisection method too, where we tighten the length of the interval containing the solution of $\delta_{i-1}^{\tau} = \eta$ iteratively.

Similar to the way we prove Proposition 6.2, one can easily check that $|\tau_i(l) - \tau_i| \leqslant (t_2 - \tau_{i-1})2^{-l}$ for every $l \in \mathbb{N}$. Due to the fact that $\tau_i(l)$ converges to τ_i exponentially fast, in practice, we terminate Algorithm 2 when l is large enough and take $\tau_i(l)$ as our approximation of τ_i. •

Figure 2 shows an execution of Algorithm 1. Note that the sampling sequence obtained by the optimization algorithm is optimal for a class of disturbances (rather than for a *specific* disturbance), as defined by the cases (a), (b), and (c) in Section 3.2.

Remark 6.4. *(Generalized metric for vector-signal).* Similar to the way we define v in (40), for any $\lambda \in \{\text{pre}, \text{par}, \text{unk}\}$, we define

$$
\pi_i^\lambda \triangleq \max_{q \in [1, r(i)]_{\mathbb{N}}} \{\delta_{q,i}^\lambda\},
$$

Algorithm 2: Solve transcendental equation in one variable

Data: Derivative bound signal y_d, τ_{i-1} and t_2
Result: τ_i that satisfies $\delta^{\tau}_{i-1} = \eta$
Initialization: $c(0) = \tau_{i-1}$, $d(0) = t_2$, and $\tau_i(0) = (c(0)+d(0))/2$
while *true* **do**
  if $(\tau_i(l) - \tau_{i-1}) \max_{t\in[\tau_{i-1},\tau_i(l)]}\{y_d(t)\} > \eta$ **then**
    $c^{l+1} = c^l$, $d^{l+1} = \tau_i(l)$
  else
    $c^{l+1} = \tau_i(l)$, $d^{l+1} = d^l$
  end
  $\tau_i(l) = (c^{k+1} + d^{k+1})/2$ and $l = l+1$
end

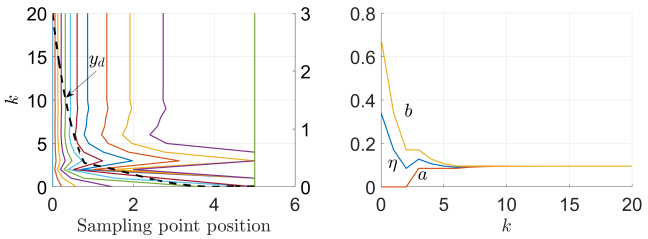

(a) (b)

Figure 2. Execution of Algorithm 1. Here $y : \mathbb{R} \to \mathbb{R}$, $t \mapsto e^{-2t} + \sin t e^{-t} K$, with $|K| \leqslant 1$. One can easily check that $y_d : \mathbb{R} \to \mathbb{R}_{\geqslant}$, $t \to 2|e^{-2t}| + |\cos t e^{-t} - \sin t e^{-t}|$ satisfies $|\dot{y}(t)| \leqslant y_d(t)$ for any $t \geqslant 0$. The interval of interest is determined by $t_1 = 0$, $t_2 = 5$. We run the algorithm for $r = 12$ sampling points and set $v^{\text{err}} = 2^{-19} v(\tau^{\text{even}})$. (a) shows y_d and the trajectories of the 12 sampling points at each iteration. Since y_d is monotonically decreasing, as k increases, τ^k tends to be dense around $t = 0$s and sparse around $t = 5$s. (b) shows the convergence of a^k, b^k and η^k.

$$\pi^{\lambda} \triangleq \max_{i\in[1,m+n]_{\mathbb{N}}} \{\pi_i^{\lambda}/(x_i^{\max} - x_i^{\min})\}, \tag{44}$$

and use π^{λ} as the metric measuring the approximation gap between Ψ_I^{λ} (resp. Ψ_O^{λ}) and Ψ^{λ} (resp. $\Psi_{\text{cl}}^{\lambda}$), where the coefficient $1/(x_i^{\max} - x_i^{\min})$ scales π_i^{λ} relative to its bounds. One can reduce π^{λ} by applying Algorithm 1 component-wise to optimize the sampling sequence τ^i for each $i \in [1, m+n]_{\mathbb{N}}$. •

7 Simulations

Here we illustrate our results on the IEEE 39-bus New England power network displayed in Figure 3. This network has 46 transmission lines and 10 generators serving a load of approximately 6GW. We run our simulations in MATLAB on a desktop with a 3.5GHz Intel Core i7-4770k quad-core CPU and 8GB of RAM. For system (2), the susceptance b_{ij} and the rotational inertia M_i for generator nodes are taken from the Power System Toolbox [35]. We assign all non-generator buses an uniform small inertia $M_i = 0.1$. Let the damping parameter (or droop coefficient) to be $D_i = 1$ for all buses. The nominal power injection $P^{\text{nom}}(t)$ is chosen to be a constant P_0 obtained from the same toolbox. The initial state $(\Lambda(0), \Omega(0))$ is chosen to be the equilibrium with respect to the input $P(t) = P_0$. The frequency bounds are $F^{\max} = -F^{\min} = 10$ unit $\times \mathbf{1}_{46}$, the power flow bounds are $\Omega^{\max} = -\Omega^{\min} = 0.5$ Hz $\times \mathbf{1}_{39}$, and the time period considered for transient-safety is $[t_1, t_2] = [0, 3]$. If there is no disturbance injection, then the state $(\Lambda(t), \Omega(t))$ stays at equilibrium, which trivially satisfies the transient-safety requirements.

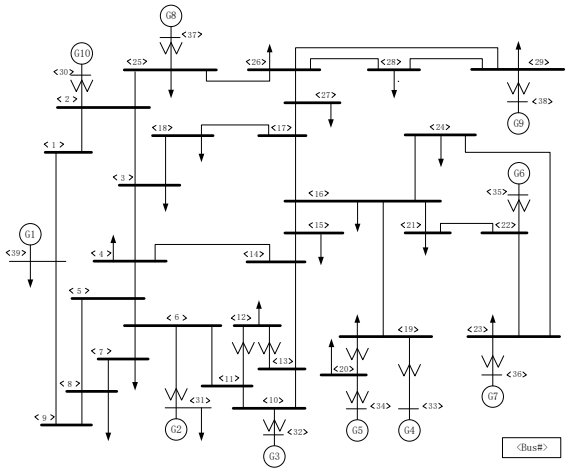

Figure 3. IEEE 39-bus power network.

We start by showing the efficiency of the approximation gap reduction obtained by Algorithm 1. We consider the case when a precisely known disturbance occurs at the 16th and the 24th buses, with the trajectory form of a step signal. Formally, this corresponds to the model (4) with $B \in \mathbb{R}^{39\times 2}$, where $B_{ij} = 1$ only when (i, j) equals $(16, 1)$ and $(24, 2)$; $\text{diag}(\zeta^{\text{pre}}(t)) = \text{diag}([1(t)\ \ 1(t)])$, and $K^{\text{pre}} = [K_1^{\text{pre}}\ \ K_2^{\text{pre}}]$ for which the bound $\gamma^{\text{pre}} = 4.7$ is known. We compute the approximations Ψ_I^{pre} and Ψ_O^{pre} using the expressions (35) in Theorem 5.5. We use the same sampling sequence for each component $i \in [1, m+n]_{\mathbb{N}}$ and consider two cases: an even sampling sequence of period $0.02s$ and the sequence that results from optimizing it by applying Algorithm 1. Figure 4(a) and (b) show the approximation sets Ψ_O^{pre} and Ψ_I^{pre} obtained in each case, with a marked improvement in the case of the optimized sequence. Figure 4(c) shows the result obtained with an optimized sequence using Algorithm 1 on an even sampling sequence of period 0.01s. The gap between the two approximation sets is smaller than in Figure 4(b), which is in agreement with the convergence result in Theorem 5.5(ii).

Figure 5 illustrates how the trajectory form impacts the shape and size of the tolerableness set. Figure 5(a) shows the inner and outer approximations when the step function in the first component of the disturbance trajectory is delayed by one second, i.e., $\zeta^{\text{pre}}(t) = [1(t-1)\ \ 1(t)]^T$. Figure 5(b) shows the same sets when the trajectory form is the sinusoid $\zeta^{\text{pre}}(t) = [\sin(\pi t)\ \ \sin(\pi t)]^T$. Comparing with Figure 4(c), one observes that the tolerableness set can take remarkably different forms depending on the type of disturbance (even though all the three trajectory forms are bounded by 1).

Next, we illustrate the containment relations among the approximations and the exact tolerableness set stated in Theorem 5.5(i). To do this, we select two nearby disturbance amplitudes, $K_I^{\text{pre}} = [2\ \ -3]^T \in \Psi_I^{\text{pre}}$ and $K_O^{\text{pre}} = [2\ \ -3.1]^T \notin \Psi_O^{\text{pre}}$. Figure 6 shows the state trajectories of (2) corresponding to each disturbance. In the case of K_I^{pre}, the frequency responses (resp. flow responses) of all buses (resp. transmission lines) stay within the ± 0.5Hz (resp. ± 10unit) bound, and hence $K_I^{\text{pre}} \in \Psi^{\text{pre}}$ according to (5), which is consistent with the inclusion $\Psi_I^{\text{pre}} \subseteq \Psi^{\text{pre}}$.

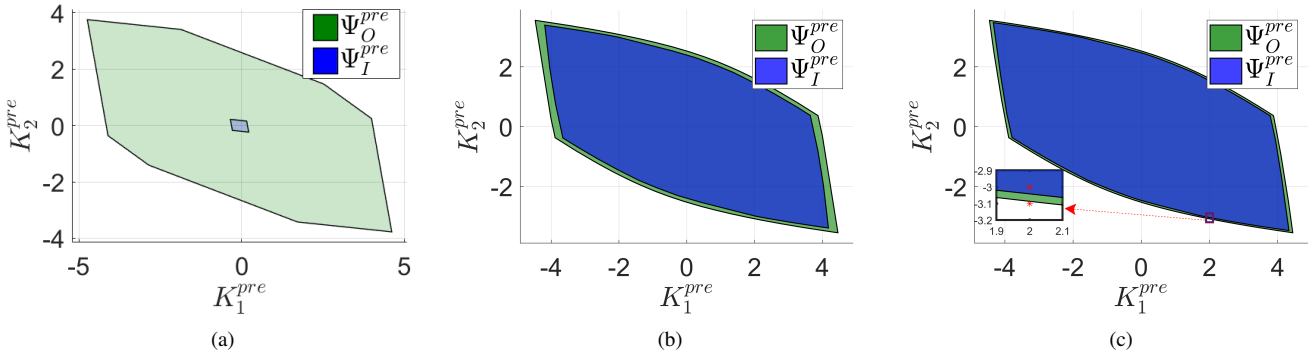

Figure 4. Inner and outer approximations of the transient-state tolerableness set for the precisely known case with different sampling sequences. Plot (a) uses even sampling with 151 points. Plots (b) and (c) use optimized sampling sequences with 151 and 301 points, respectively. The first two plots show that Algorithm 1 reduces the gap between the inner and outer approximations for a fixed number of sampling points. The last two plots illustrate the convergence of the approximations as the number of sampling points increases.

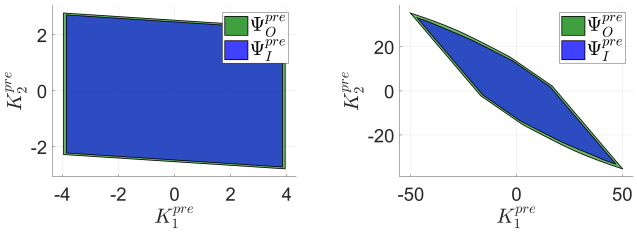

Figure 5. Inner and outer approximations of transient-state tolerableness set for the precisely known case with different trajectory forms. In plot (a), the trajectory form is $\zeta^{\text{pre}}(t) = [1(t-1s)\ 1(t)]^T$ and in plot (b) $\zeta^{\text{pre}}(t) = [\sin(\pi t)\ \sin(\pi t)]^T$, respectively.

Sets	Time(s)	Sets	Time(s)
Figure 4(a)	12.41	Figure 5(a)	18.62
Figure 4(b)	14.39	Figure 5(b)	16.52
Figure 4(c)	20.38	Figure 7(a) and (b)	20.26 and 20.39

Table 1
Times for the computation of for various tolerableness sets.

In the case of K_O^{pre}, one frequency response goes beyond the -0.5Hz bound, reaching to approximately -0.506Hz, violating the frequency safety requirement slightly, and hence $K_O^{\text{pre}} \notin \Psi_{\text{cl}}^{\text{pre}}$, which is consistent with the inclusion $\Psi_{\text{cl}}^{\text{pre}} \subseteq \Psi_O^{\text{pre}}$.

Figure 7 illustrates the computation of the inner and outer approximation sets in the cases when the disturbance trajectory form is partially known and unknown. In the first case, for the model (6), we have the nominal trajectory form $\zeta^{\text{nom}}(t) = 0.9 \cdot [1(t)\ 1(t)]^T$ and the uncertainty bound $\alpha = 0.1 \cdot \mathbf{1}_2$ on ζ^{err}. Since $|\zeta^{\text{pre}}(t) - \zeta^{\text{nom}}(t)| \leqslant \alpha$ and $|\zeta^{\text{nom}}(t)| + \alpha \leqslant 1$ for every $t \in [t_1, t_2]$, we deduce from Remark 4.2 that $\Psi^{\text{unk}} \subset \Psi^{\text{par}} \subset \Psi^{\text{pre}}$. The comparison of Figures 4 and 7 validates these containment relations.

Table 1 gathers the computational time for the inner and outer approximations in Figures 4, 5 and 7. The additional 2 seconds for Figure 4(b) with respect to Figure 4(a) are due to the take taken by the optimization of the sampling sequence. This latter time increases as more sampling points are considered, cf. Figure 4(c). We also see a slight computational time difference among Figure 4(c), Figure 5(a), and Figure 5(c), corresponding to different disturbance trajectory forms. Finally, for a fixed number of sampling points, the computational time does not vary dramatically for precisely known, partially known, and totally unknown disturbances. Computational times are also reported in [1] for a simulation on the IEEE 118-bus network with 91 disturbances.

Finally, we illustrate the robustness metric definition based on tolerableness sets introduced in by Remark 5.8. We consider 39 different scenarios: in the ith scenario, we inject a power disturbance with trajectory form $1(t)$ only at node i. For each $i \in \{1, \cdots, 39\}$, β_O^{pre} (resp. β_I^{pre}) stands for the upper (resp. lower) approximation of the maximum allowable disturbance magnitude injected at node i so that the whole network maintains transient-state safety. One can see from Figure 8 that nodes $1, 9, 12$ and 38 are the most vulnerable. The first three cases have similar causes – either low inertia, making the transient frequency easily affected by disturbances or low dissipation capabilities due to a small number of neighboring nodes, resulting in a relatively long time required to dissipate the disturbances. The 38th node case is primarily due to the fact that the only transmission line connecting the node with the rest of the network is almost saturated before the disturbance injection.

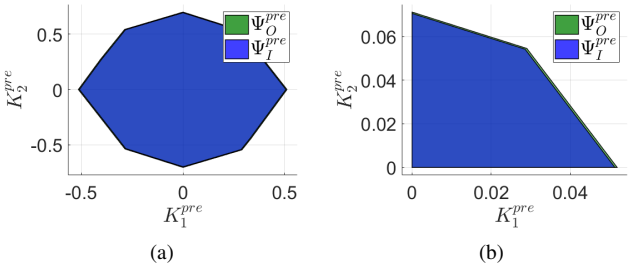

Figure 7. Inner and outer approximations of the transient-state tolerableness set with partially known and totally unknown trajectory forms. Plot (a) shows the tolerableness set with nominal trajectory form $\zeta^{\text{nom}}(t) = 0.9 \cdot [1(t)\ 1(t)]^T$ and uncertainty $\alpha = 0.1 \cdot \mathbf{1}_2$. Plot (b) shows the set with totally unknown trajectory. Together with Figure 4(c) one has that $\Psi^{\text{unk}} \subseteq \Psi^{\text{par}} \subseteq \Psi^{\text{pre}}$, as stated in Remark 4.2.

8 Conclusions

We have considered the problem of efficiently describing the set of disturbances to a power network that do not affect its transient-

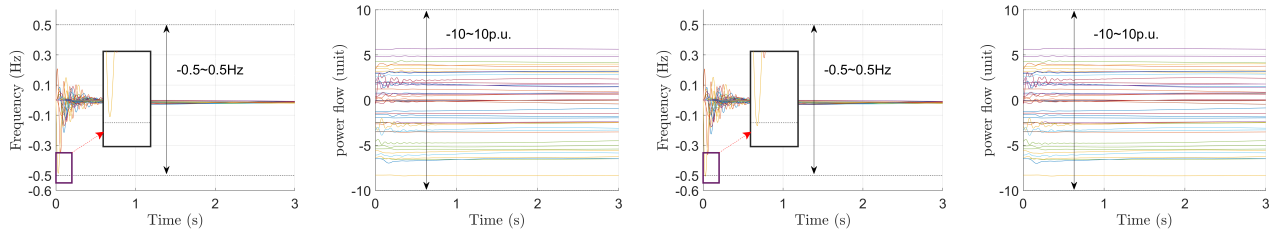

(a) (b) (c) (d)

Figure 6. Frequency and power flow trajectories with different disturbance amplitudes. The problem data is the same as in Figure 4. Plots (a) and (b) show the trajectories with a disturbance amplitude $K_I^{\text{pre}} = [2\ -3]^T$ (which, from Figure 4(c), is contained in the inner approximation set Ψ_I^{pre}), while plots (c) to (d) show the trajectories for $K_O^{\text{pre}} = [2\ -3.1]^T$ (which is not contained in the outer approximation set Ψ_O^{pre}). In both cases, the power flow trajectories stay within the ± 10 unit bound. However, all the frequency trajectories stay within the ± 0.5 Hz bound when the disturbance amplitude is K_I^{pre}, while for the K_O^{pre}case, one frequency trajectory hits up to approximately -0.506Hz, exceeding the -0.5Hz bound.

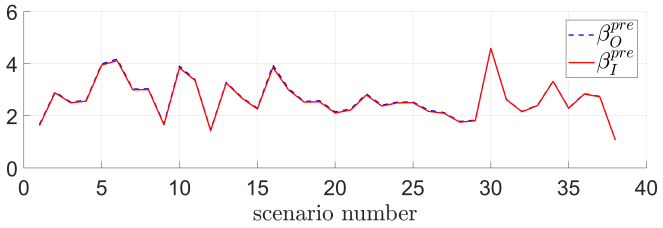

Figure 8. Robustness characterization of the IEEE39 bus network based on tolerableness sets. In each scenario, we inject a disturbance at the corresponding node and compute the approximations of the robustness metric defined in Remark 5.8. This metric measures the maximum allowable disturbance that does not violate transient safety. Both approximations use 301 sampling points optimized through Algorithm 1.

state safety in terms of frequency and power flow. Under the assumption that a bound on the amplitude of the disturbance is available, we have devised a sampling method to provide inner and outer approximations of the transient-state tolerableness set. These approximations can be computed with arbitrary accuracy, at the cost of increasing the computational complexity. We have also introduced a metric to measure the approximation gap and designed an algorithm to optimize it for a given fixed number of sampling points. Future work will extend the analysis from unknown constant amplitude to unknown time-varying amplitude, and quantify the difference between the tolerableness sets of the nonlinear swing dynamics and its linearized version.

REFERENCES

[1] Y. Zhang and J. Cortés, "Transient-state feasibility set approximation of power networks against disturbances of unknown amplitude," in *American Control Conference*, Seattle, WA, May 2017, pp. 2767–2772.

[2] P. Kundur, J. Paserba, V. Ajjarapu, G. Andersson, A. Bose, C. Canizares, N. Hatziargyriou, D. Hill, A. Stankovic, C. Taylor, T. V. Cutsem, and V. Vittal, "Definition and classification of power system stability," *IEEE Transactions on Power Systems*, vol. 19, no. 2, pp. 1387–1401, 2004.

[3] A. Gajduk, M. Todorovski, and L. Kocarev, "Stability of power grids: an overview," *The European Physical Journal Special Topics*, no. 223, pp. 2387–2409, 2014.

[4] I. Nagel, L. Fabre, M. Pastre, F. Krummenacher, R. Cherkaoui, and M. Kayal, "High-speed power system transient stability simulation using highly dedicated hardware," *IEEE Transactions on Power Systems*, vol. 28, no. 4, pp. 4218–4227, 2013.

[5] A. S. Deese and C. O. Nwankpa, "Utilization of FPAA technology for emulation of multiscale power system dynamics in smart grids," *IEEE Transactions on Smart Grid*, vol. 2, no. 4, pp. 606–614, 2011.

[6] R. Fried, R. S. Cherkaoui, C. C. Enz, A. Germond, and E. A. Vittoz, "Approaches for analog VLSI simulation of the transient stability of large power networks," *IEEE Transactions on Circuits and Systems I: Fundamental Theory and Applications*, vol. 46, no. 10, pp. 1249–1263, 1999.

[7] M. Pavella, D. Ernst, and D. Ruiz-Vega, *Transient Stability of Power Systems: A Unified Approach to Assessment and Control*. Kluwer Academic Publishers, 2012.

[8] A. Pai, *Energy Function Analysis for Power System Stability*. Springer, 1989.

[9] H.-D. Chiang, F. F. Wu, and P. P. Varaiya, "A BCU method for direct analysis of power system transient stability," *IEEE Transactions on Power Systems*, vol. 9, no. 3, pp. 1194–1208, 1994.

[10] M. Anghel, F. Milano, and P. Antonis, "Algorithmic construction of Lyapunov functions for power system stability analysis," *IEEE Transactions on Circuits and Systems I: Regular Papers*, vol. 60, no. 9, pp. 2533–2546, 2013.

[11] F. Dörfler and F. Bullo, "Synchronization and transient stability in power networks and nonuniform Kuramoto oscillators," *SIAM Journal on Control*, vol. 50, no. 3, pp. 1616–1642, 2012.

[12] T. L. Vu, S. M. A. Araifi, M. S. E. Moursi, and K. Turitsyn, "Toward simulation-free estimation of critical clearing time," *IEEE Transactions on Power Systems*, vol. 31, no. 6, pp. 4722–4731, 2016.

[13] Y. Zhang and J. Cortés, "Quantifying the robustness of power networks against initial failure," in *European Control Conference*, Aalborg, Denmark, July 2016, pp. 2072–2077.

[14] Q. Ba and K. Savla, "On distributed computational approaches for optimal control of traffic flow over networks," in *Allerton Conf. on Communications, Control and Computing*, Monticello, IL, 2016, pp. 1102–1109.

[15] S. Soltan, D. Mazauric, and G. Zussman, "Analysis of failures in power grids," *IEEE Transactions on Control of Network Systems*, vol. 4, no. 2, pp. 288–300, 2017.

[16] Y. Yang, T. Nishikawa, and A. E. Motter, "Small vulnerable sets determine large network cascades in power grids," *Science*, vol. 358, no. 6365, 2017.

[17] I. M. Mitchell, "Comparing forward and backward reachability as tools for safety analysis," in *Hybrid Systems: Computation and Control*. Springer, 2007, pp. 428–443.

[18] M. Kloetzer and C. Belta, "Reachability analysis of multi-affine systems," in *Hybrid Systems: Computation and Control*, ser. Lecture Notes in Computer Science, J. P. Hespanha and A. Tiwari, Eds. Santa Barbara, CA: Springer, 2006, vol. 3927, pp. 348–362.

[19] T. Dang, "Approximate reachability computation for polynomial systems," in *Hybrid Systems: Computation and Control*, ser. Lecture Notes in Computer Science, J. P. Hespanha and A. Tiwari, Eds. Santa Barbara, CA: Springer, 2006, vol. 3927, pp. 138–152.

[20] Y. C. Chen and A. D. Domínguez-García, "A method to study the effect of renewable resource variability on power system dynamics," *IEEE Transactions on Power Systems*, vol. 27, no. 4, pp. 1978–1989, 2012.

[21] H. N. Villegas-Pico and D. C. Aliprantis, "Voltage ride-through capability verification of wind turbines with fully-rated converters using reachability analysis," *IEEE Transactions on Energy Conversion*, vol. 29, no. 2, pp. 392–405, 2014.

[22] A. El-Guindy, D. Han, and M. Althoff, "Formal analysis of drum-boiler units to maximize the load-following capabilities of power plants," *IEEE Transactions on Power Systems*, vol. 31, no. 6, pp. 4691–4702, Jan. 2016.

[23] A. El-Guindy, K. Schaab, B. Schürmann, O. Stursberg, and M. Althoff, "Formal LPV control for transient stability of power systems," in *Power and Energy Society General Meeting (PESGM)*, 2018, pp. 1–5.
[24] H. Choi, P. J. Seiler, and S. V. Dhople, "Propagating uncertainty in power-system DAE models with semidefinite programming," *IEEE Transactions on Power Systems*, vol. 32, no. 4, pp. 3146–3156, 2016.
[25] F. Bullo, J. Cortés, and S. Martínez, *Distributed Control of Robotic Networks*, ser. Applied Mathematics Series. Princeton University Press, 2009, electronically available at http://coordinationbook.info.
[26] N. Biggs, *Algebraic Graph Theory*, 2nd ed. Cambridge University Press, 1994.
[27] S. I. Resnick, *A Probability Path*. Birkhäuser Boston, 1998.
[28] M. Rohden, A. Sorge, M. Timme, and D. Witthaut, "Self-organized synchronization in decentralized power grids," *Physical Review Letters*, vol. 109, no. 6, p. 064101, 2012.
[29] T. S. Borsche, T. Liu, and D. J. Hill, "Effects of rotational inertia on power system damping and frequency transients," in *IEEE Conf. on Decision and Control*, Osaka, Japan, 2015, pp. 5940–5946.
[30] S. Sastry and P. Varaiya, "Hierarchical stability and alert state steering control of interconnected power systems," *IEEE Transactions on Circuits and Systems*, vol. 27, pp. 1102–1112, 1980.
[31] C. Zhao, U. Topcu, N. Li, and S. H. Low, "Design and stability of load-side primary frequency control in power systems," *IEEE Transactions on Automatic Control*, vol. 59, no. 5, pp. 1177–1189, 2014.
[32] P. Kundur, *Power System Stability and Control*. McGraw-Hill, 1994.
[33] N. W. Miller, M. Shao, and S. Venkataraman, "California ISO (CAISO) frequency response study," General Electric International, Inc, Tech. Rep., 2011.
[34] M. H. Protter and C. B. J. Morrey, *A First Course in Real Analysis*, 2nd ed., ser. Undergraduate Texts in Mathematics. New York: Springer, 1997.
[35] K. W. Cheung, J. Chow, and G. Rogers, *Power System Toolbox, v 3.0.* Rensselaer Polytechnic Institute and Cherry Tree Scientific Software, 2009.

Yifu Zhang received the B.S. degree in automatic control from the Harbin Institute of Technology, China, in 2010. He is currently pursing the Ph.D. degree in mechanical and aerospace engineering at the University of California, San Diego. His research interests include power grid analysis, distributed coordination algorithms, model predictive control, and adaptive control.

Jorge Cortés (M'02, SM'06, F'14) received the Licenciatura degree in mathematics from Universidad de Zaragoza, Zaragoza, Spain, in 1997, and the Ph.D. degree in engineering mathematics from Universidad Carlos III de Madrid, Madrid, Spain, in 2001. He held postdoctoral positions with the University of Twente, Twente, The Netherlands, and the University of Illinois at Urbana-Champaign, Urbana, IL, USA. He was an Assistant Professor with the Department of Applied Mathematics and Statistics, University of California, Santa Cruz, CA, USA, from 2004 to 2007. He is currently a Professor in the Department of Mechanical and Aerospace Engineering, University of California, San Diego, CA, USA. He is the author of Geometric, Control and Numerical Aspects of Nonholonomic Systems (Springer-Verlag, 2002) and co-author (together with F. Bullo and S. Martínez) of Distributed Control of Robotic Networks (Princeton University Press, 2009). He was an IEEE Control Systems Society Distinguished Lecturer (2010-2014). His current research interests include cooperative control, network science, game theory, multi-agent coordination in robotics, power systems, and neuroscience, geometric and distributed optimization, nonsmooth analysis, and geometric mechanics and control.